Artificial Co-Drivers as a Universal Enabling Technology for Future Intelligent Vehicles and Transportation Systems

Mauro Da Lio, *Member, IEEE*, Francesco Biral, Enrico Bertolazzi, Marco Galvani, Paolo Bosetti, David Windridge, Andrea Saroldi, and Fabio Tango

***Abstract*—This position paper introduces the concept of artificial "co-drivers" as an enabling technology for future intelligent transportation systems. In Sections I and II, the design principles of co-drivers are introduced and framed within general human–robot interactions. Several contributing theories and technologies are reviewed, specifically those relating to relevant cognitive architectures, human-like sensory-motor strategies, and the emulation theory of cognition. In Sections III and IV, we present the co-driver developed for the EU project interactIVe as an example instantiation of this notion, demonstrating how it conforms to the given guidelines. We also present substantive experimental results and clarify the limitations and performance of the current implementation. In Sections IV and V, we analyze the impact of the co-driver technology. In particular, we identify a range of application fields, showing how it constitutes a universal enabling technology for both smart vehicles and cooperative systems, and naturally sets out a program for future research.**

***Index Terms*—Advanced driver assistance systems (ADAS), artificial cognitive systems, emulation theory of cognition, intelligent vehicles, man–machine systems, optimal control (OC).**

I. Introduction—Toward Human Peer Vehicles

RESEARCH in intelligent transportation systems began in the late 1980s with the PATH program in the United States, the PROMETHEUS project in the EU, and the ASV projects in Japan. While one line of research centered on fully autonomous vehicles, the vast majority of research projects has focused on driver assistance systems [1], [2] as a recognized component of vehicle–human interaction research. The principles of smart collaboration between humans and systems have been the focus of a number of theoretical studies, such as those by Inagaki [3], Flemisch *et al.* [4], Norman [5], Heide and Henning [6], Li *et al.* [7], and others, which may include full automation as one extreme point of the interaction spectrum [8].

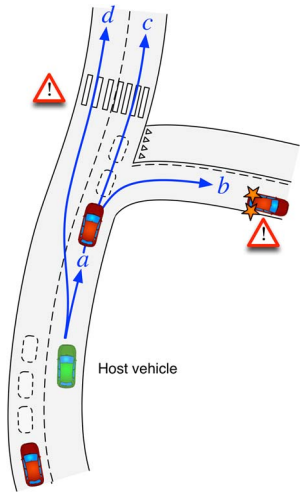

Fig. 1. Example scenario: The host vehicle travels in traffic that exhibits potentially dangerous locations, complex road features, and multiple possible goals.

A. Introducing Co-Drivers

Fig. 1 describes an example situation of typical complexity.

One main focus of this paper will be to identify a technological roadmap that is capable of giving rise to smart collaborative control of the types described in [3]–[7]. With this respect, Wang's multiagent framework of "simple inside vehicles, complex outside vehicles" and ACP-based parallel approach of "actual versus artificial" are also closely relevant [9], [10].

For the purpose of this paper, we first address the preliminary question:

How would a human driver drive?

Depending on its application context, a system capable of determining how an *expert human* would drive could be regarded either as a kind of "holistic driver model" or as an "artificial human-like driver." (For readers interested in the state-of-the-art of driver modeling, reviews are given in [11] and [12].)

Such an artificial driver would be sufficient for developing autonomous vehicles that move and react as if driven by a human. However, this would still be insufficient, in itself, for developing meaningful interactions with a human driver.

Manuscript received November 1, 2013; revised February 28, 2014, April 29, 2014, and June 2, 2014; accepted June 6, 2014. Date of publication July 11, 2014; date of current version January 30, 2015. This work was supported by the European Commission under Grants FP6 507075 (PReVENT), FP7 216355 (SAFERIDER), FP7 246587 (interactIVe), and FP7 215078 (DIPLECS). The Associate Editor for this paper was L. Li.

M. Da Lio, F. Biral, E. Bertolazzi, M. Galvani, and P. Bosetti are with the Department of Industrial Engineering, University of Trento, 38123 Trento, Italy (e-mail: mauro.dalio@unitn.it; francesco.biral@unitn.it; enrico.bertolazzi@unitn.it; paolo.bosetti@unitn.it; marco.galvani@unitn.it).

D. Windridge is with the Centre for Vision Speech and Signal Processing, University of Surrey, Surrey GU2 7XH, U.K. (e-mail: D.Windridge@surrey.ac.uk).

A. Saroldi and F. Tango are with the Centro Ricerche Fiat, 10043 Orbassano, Italy (e-mail: andrea.saroldi@crf.it; fabio.tango@crf.it).

Color versions of one or more of the figures in this paper are available online at http://ieeexplore.ieee.org.

Digital Object Identifier 10.1109/TITS.2014.2330199

1524-9050 © 2014 IEEE. Translations and content mining are permitted for academic research only. Personal use is also permitted, but republication/redistribution requires IEEE permission. See http://www.ieee.org/publications_standards/publications/rights/index.html for more information.

On inspection of Fig. 1, it is clear that we cannot easily tell how a human would drive without knowing his/her *goal/intentions*. In fact, a human would drive in distinctly different ways depending on whether his/her goal is d, or $a-c$, or $a-b$.

Definition: We therefore conceive the notion of a "*co-driver*": an artificial agent that is able *both* to drive similar to a human *and* to infer human intentions, interacting accordingly, including rectifying mistakenly executed actions by the human driver.

II. Co-Driver Enabling Technologies

A. Natural Co-Drivers

We note that "natural" co-drivers already exist. A driving license tutor would be a first obvious example: The tutor has knowledge of human motion schemes and is able to infer the trainee's intentions, thus acting on the vehicle controls in accordance with the trainee's needs, given the context.

In colloquial terms, it is obvious that the human co-driver can "understand" the trainee. How this actually happens will be a central concern for the agent development arguments set out below.

Note that this co-driver relationship is not limited to human intelligences. The rider–horse metaphor (or H-metaphor) describes a *symbiotic system*, in which an animal can "read" human intentions, and, reciprocally, the rider can "read" the animal's intentions [4], [5], with the horse seeking to maximally reduce the human's riding burdens consistent with their intentions.

B. Architectural Considerations

The first consideration concerns the agent architecture. Let us first consider the so-called "*sense–think–act*" architecture [see Fig. 2(a)], which has been often used in driver assistance systems (e.g., *perception–situation assessment–action*). This architecture corresponds to the traditional view of psychology and artificial intelligence [13]–[15], known also as the *computer metaphor*, which divides the agent's functioning into sequential steps. The scope of perception in this context is thus making an "internal model" of the world, which is thereafter symbolically manipulated by a "mind," and subsequently fed into an output buffer. Internal models have been introduced since the works of Craik [16] and Newell and Simon [14] to explain how agents may *act beyond simply reactive behaviors*, such as making plans for things that they cannot currently sense.

A contrasting view is the *behavioral* architecture introduced by Brooks [17] [see Fig. 2(b)]. This architecture starts with simple sensory-motor loops, representing elementary behaviors (e.g., obstacle avoidance) and grows by adding behavioral layers that *subsume* the already implemented layers to achieve newer and more complex functions. In contrast to the sense–think–act architecture, the agent is here decomposed by horizontal levels of competence enacted via control loops without explicit internal models of the world.

Brook's architecture is one of the many new ideas that, since late 1980s, challenged the traditional view of cognition (the computer metaphor), along with connectionism, ethological approaches, adaptive behaviors, dynamic systems theory, etc., together constituting the so-called *embodied situated cognitive science* approach [18]–[32]. According to these, cognition arises from the interaction of the agent with the environment, with action typically preceding perception, and driving the evolution of the agent [see Fig. 2(b)].

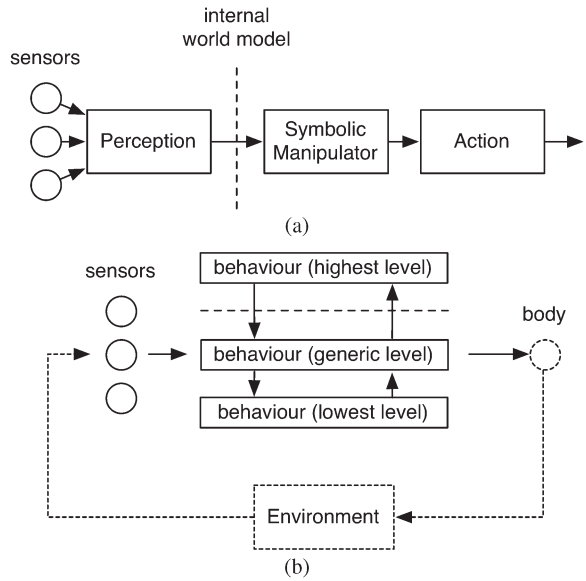

Fig. 2. (a) The traditional view of cognition decomposes agents in sequential steps, e.g., *sense–think–act*. (b) The embodied cognition paradigm sees agents as *perception–action behaviors* organized in hierarchies, with higher levels subsuming lower levels, that are produced as the agent evolves via interaction with its own body and the environment.

The two contrasting views have been extensively debated, not only in terms of questioning the idea of cognition as amodal symbol manipulation but also in terms of the related concept of "internal (symbolic) representation" [32]–[40]. Although some researchers supported the idea of "intelligence without *any* representation" at all (e.g., [21], [29], and [32]), other researchers have developed novel concepts of "representation" [33]–[39] among which *emulators* [40], [41], which can be used for anticipation of sensory input, predictive and optimal control (traits that have been long recognized in driver models [11], [12]), deliberation (going beyond reactive behavior), imitation, learning, empathy, mind reading, and cooperation [42]–[62] (e.g., see a review by Hesslow [45]).

The sense–think–act architecture (in the form *perception–situation assessment–action*) has hitherto been the natural choice for systems that were fully engineered by design, as is the case for most driver assistance systems. For example, the authors employed it in the PReVENT project [63], [64]. However, as the complexity of the driver support function grew, the known shortcomings of this type of architecture [17] became evident (particularly in terms of scalability, maintainability, flexibility, and robustness).

The behavioral architecture has also been used in intelligent vehicles, particularly within the project DIPLECS [65], which adopted the architecture in Fig. 2(b), with layers inspired by the Extended Control Model (ECOM) [66]–[68], which is a psychological driver model that seeks to explain driving as a

hierarchy of concurrent subsumptive control loops that execute at progressively decreasing time scales (i.e., such that the more abstract layers typically operate over longer time scales). DIPLECS implemented the three bottom-most ECOM layers: *tracking* (minute chassis control and disturbance rejection), *regulating* (producing space–time trajectories), and *monitoring* (keeping track of the progress toward the destination and setting related short-term goals, e.g., overtaking). Each layer was built from *learned perception–action* cycles [69]–[77].

C. Empathic Link and Joint Action

The *Simulation Theory of Cognition* is a conceptual framework [45] that essentially states that "thinking is simulation of perception and action," carried out as covert motor-sensory activity, e.g., [42], [46], and [50].

In this framework, the understanding of others' intentions is also a simulation process, carried out via the "mirroring" of observed motor activities of the others, e.g., [43], [51], [52], [62] (colloquially speaking: "standing in the shoes of others"). The "like me" framework [62] for understanding others' intentions is summarized by Meltzoff as: "others who act like me have internal states like me."

Not only are humans skilled in the latter but they can also intrinsically *correct mistakes* in the execution of tasks while preserving the ultimate goal. For example, in the experiment reported by Meltzoff, 18-month-old children are able to correctly execute a task that has been incorrectly demonstrated [61].

Inference of intentions has also been further studied by Wolpert *et al.* [52], [53], [60], [78], [79] and Demiris *et al.* [55]–[59], [80], [81]: Their approach is to *generate* agent behaviors under a number of alternative hypotheses, which are then tested by comparison with observed behaviors. This means that "multiple simulations" are run in parallel, and the most salient one(s) are selected. This method is termed the "generative" approach.

Hurley, in 2008, combined many ideas into an interpretative scheme named the Shared Circuit Model [51]. In the following, we adopt Hurley's picture as a useful frame of reference.

In broad terms, Fig. 3 indicates an agent capable of interacting with the environment (the outer dashed loop) in agreement with the embodied cognition approach. However, in the Hurley model, details are also provided for the *inner structure* of the agent.

The main element is the existence of an internal loop that goes backwards from action to perception. This posited loop is a *forward emulator*, which simulates the effect of agent motor activity as *if it were* produced in actuality (a key contribution here is due to Grush [40]). In overt motor activities, these cerebellar circuits [41], fed by "efference" copies of the motor commands, anticipate sensory input. A parallelism with control theory can be drawn, where predictive models can be used to stabilize sparse noisy sensory input (by analogy to Kalman filters), to enhance the processing of sensorial information, as trackers (retaining awareness of things coming into and out of the senses), and to implement efficient (model) predictive control. The usefulness of forward emulators extends to covert motor activities, where they may be *used offline* to produce motor imagery; to estimate the effect of hypothetical actions; to develop and evaluate plans, such as model-based planning in control theory (e.g., model-predictive control and Optimal Control); and finally, to simulate the observed actions of other people.

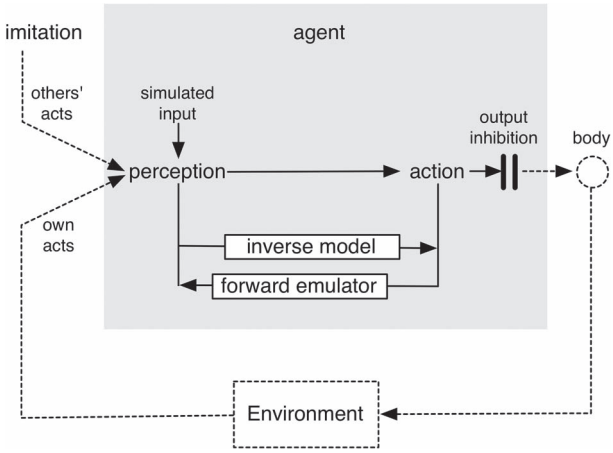

Fig. 3. Architecture of a cognitive agent equipped with emulation and mirroring, capable of imitation, mind reading, and deliberation (the Share Circuit Model, see text).

D. Sensory-Motor Cycles That are "Human-Like"

Many researchers have focused on human movement and on how it accords to efficiency principles built in the central nervous system. In this respect, Todorov *et al.* [82]–[84], Wolpert *et al.* [79], [85], Harris [86], [87], Viviani and Flash [88], Flash *et al.* [89]–[91], and many others (going back to the 1970s) show evidence that biological beings move according to optimal criteria. In particular, Harris and Wolpert indicate minimization of postmovement errors and rejection of neural noise (the "minimum variance" principle) to be the underlying efficiency criterion, capable of explaining observed human time–accuracy tradeoff and the so-called "two-thirds power law" (see below).

Optimal Control is thus a convenient means to reproduce simple sensory-motor primitives, e.g., as demonstrated in [83] and [92]. Optimal inverse emulators (see Fig. 3) may be derived with this principle.

Application of OC within a receding-horizon scheme explains another observed fact, known as the "minimum intervention principle" [93], [94], which states that *task-irrelevant* deviations are left uncorrected.

Viviani and Flash [88], Flash *et al.* [89], [91], and others also showed that lateral acceleration and speed in human movements are inversely correlated with curvature (the "two-thirds power law"), which Harris explains as a consequence of the minimum variance principle. Within driving, an analogous phenomenon exists: Ordinary drivers use lateral acceleration and speed in inverse correlation with road curvature (far below that appropriate to friction limits on dry roads and, thus, unrelated to it). This phenomenon was independently observed and called the "willingness envelope" in [95]–[98]. In [98], Bosetti *et al.* demonstrate what is plausibly the same "two-thirds power law," originating from the minimum variance principle (i.e., drivers

reduce speed in curves to maintain the accuracy in lateral position).

III. Co-Driver of the Interactive Project

A. Theoretical Foundations and Design Guidelines

The main goal is to design an agent that is capable of enacting the "like me" framework, which means that it must have sensory-motor strategies *similar to that of a human* and that it must be capable of *using them to mirror* human behavior for inference of intentions and human–machine interaction.

Designing human motor strategies is a relatively easy step: One may take inspiration from human optimality motor principles. For example, we already used the minimum jerk/time tradeoff and the acceleration willingness envelope to produce human "reference maneuvers" for advanced driver assistance systems (ADAS) [63], [92], [93].

Implementing inference of intentions by mirroring, and human-peer interactions, is the second less assured step. Two notable examples (MOSAIC and HAMMER) have been mentioned for the general robotics application domain. In the driving domain, DIPLECS demonstrated learning of the ECOM structure from human-driving expert-annotated training sets, and classification of human driver states. However, no co-driver, in the sense of the definition given in Section I, has been demonstrated as yet.

The main research question and contribution of this paper is thus producing a co-driver example implementation to demonstrate the effectiveness of the simulation/mirroring mechanism and the following interactions and to focus on the important potential application impacts that follow from these.

The co-driver has been developed by a combination of direct synthesis (OC) at the motor primitive level, as well as manual tuning at higher behavioral levels (the latter being carried out after inspection of salient situations whenever the two agents happen to disagree). The final system is thus the cumulation of having compared correct human behaviors (while discarding incorrect human behaviors) with the developing agent within many situations encountered during months of development.

However, in Section VI, we describe how the same architecture can be potentially employed in the future to implement "learning by simulation," namely, optimizing higher-level behaviors with simulated interactions via the forward emulators, to let the system build knowledge automatically (instead of manually), particularly to accommodate rare events and to continuously improve its reliability.

Note that, while the main purpose of this system is "understanding" human goals for preventive safety (see below), emergency handling and efficient vehicle control intervention may be added by means of new behaviors (no longer necessarily human-like) in future versions.

B. Example Implementation

"InteractIVe" is the current flagship project of the European Commission in the intelligent vehicle domain [99]. It tackles vehicle safety in a systematic way by means of three different subprojects focusing on different time scales: from early holistic preventive safety, to automatic collision avoidance, and to collision mitigation.

Preventive safety deals with normal driving and with preventing dangerous situations. For this, a "continuous-support function" has been conceived, which monitors driving and acts whenever necessary. This functionality integrates, in a unique human–machine interaction, several distinct forms of the driver assistance system.

To implement the Continuous Support function, the co-driver metaphor was adopted. It has been implemented within four demonstrators of differing kinds. The following describes the Centro Ricerche Fiat (CRF) implementation, which is closest to the premises in Section II.

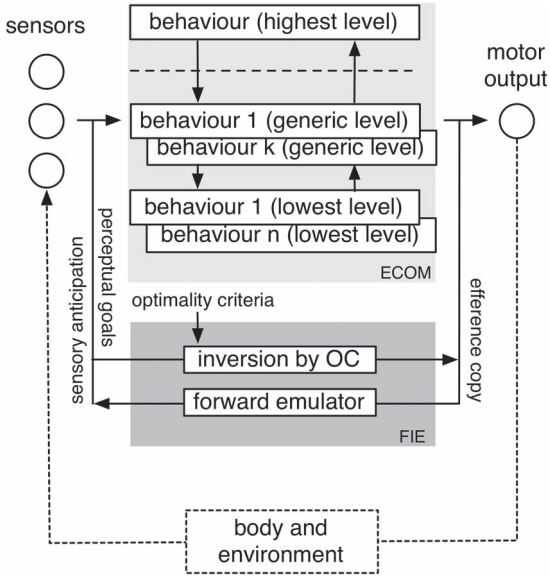

Fig. 4. Architecture of the co-driver for the CRF implementation of the Continuous Support function.

C. Co-Driver Architecture (CRF Implementation)

Fig. 4 shows the adopted architecture. The agent's "body" is the car, the agent's "environment" is the road and its users, and the "motor output" is the longitudinal and lateral control.

This architecture may be seen to resemble that in Fig. 3, albeit extended in that the perception–action link is here explicitly expanded into a subsumptive hierarchy of PA loops. As indicated in Section II, the input/output structure of layers within the subsumption hierarchy is characterized by (progressive generalizations of) perceptions and actions. The actual implementation is built up from functions with input and output characteristics described in the following section.

By comparison to Fig. 2(b), this architecture is enriched with forward/inverse models, which make it possible to operate offline for any purposes requiring "extended deliberation," e.g., for human intention recognition.

D. Building Block Details

1) Forward Emulators: While the concept of forward emulation is quite general—for instance denoting neural networks that can predict any sensory input, e.g., [40] and [41]—in our implementation, emulators are focused on a restricted domain, i.e., the prediction of the lateral and longitudinal host vehicle dynamics.

There are many vehicle dynamics models in the literature that might be adopted. Generally, they are designed to predict vehicle dynamics accurately and efficiently for the design and analysis of chassis dynamics and control systems (e.g., see classical textbooks on vehicle dynamics such as [100]).

However, the main purpose of a predictive model here is slightly different: It serves to test the viability of different hypotheses of human driving intentions. Thus, its main requirement is *similarity to humans* (if not, co-driver predictions will not match observations even for a correct hypothesis).

With these considerations in mind, we adopted the longitudinal and lateral forward emulators described in Appendix I. They are quasi-static models that ignore transient phenomena that are unlikely to be conducted by humans because of the limited frequency response of humans in either sensing or actuation. On the other hand, they capture phenomena such as sideslip and understeering, which, if otherwise ignored, would lead to a mismatch between the human and the co-driver. In other words, we make the assumption that slow, if nonlinear, phenomena are capable of being human-directed, whereas faster ones are not.

Note that we do not claim that the models given in Appendix I are necessarily the best choice. Rather, they constitute a working hypothesis to be tested. In a later section, we will discuss the strengths and limitations of this approach.

2) Inverse Models: In this implementation, inverse models are produced by means of OC. Other approaches may be based on machine learning; for example, the learning of either or both inverse and forward models, e.g., [101]–[116]. OC, with criteria derived from human movement [86], produces motor primitives that need know only the forward model (even if the forward models were learnt, we would not need to learn any corresponding inverse model).

Inverse models link perceptual goals to the actions needed to achieve those goals (see Fig. 4). For the dynamic system described in Appendix I, perceptual goals are desired states to be achieved at some time horizon T. Thus, inverse models determine the (optimal) control required to reach a desired state at some future time T. Since there may be several types of final states and optimization criteria, the inversion problem produces a corresponding number of solutions, which we may regard as different *motor primitives*.

In the proposed architecture in Fig. 4, the block labeled "inversion by OC" denotes the algorithm for solving the OC problem, whereas the lowest level behaviors of the ECOM architectures are the motor primitives, which may be conceptually thought of as instantiations of the OC problem.

3) First ECOM Layer—Motor Primitives: In the following, the motor primitives that we determined to be most useful are described.

a) Longitudinal motor primitives: Longitudinal motor primitives deal with the adaptation of speed. They are generated by the following OC problem:

Minimize the following cost functional with final time T as a *free* parameter:

$$J_s = \int_0^T w_T + j_p^2(t)\, dt \tag{1}$$

subject to:

a) The forward model, given by (A1.2) in Appendix I.
b) The initial conditions, i.e., the current state

$$s_s(0) = s_{s,0} \quad u(0) = u_0 \quad a(0) = a_0. \tag{2}$$

c) The final conditions, i.e., the motor goal. We consider two particular types of goal in the following, which produce two primitives.

The cost functional (1) is worth noting. It is formulated as a tradeoff between minimum jerk (j_p) and minimum time (w_T) to model a variety of longitudinal behaviors, from minimum effort $(w_T = 0)$, to different degrees of time constraint for execution (with ideally minimum time maneuvering for $w_T \to \infty$). Thus, w_T plays the role of a *motivation parameter*, modeling how fast the intention can be executed or the tradeoff between speed and accuracy inherent in any human movement.

Speed Matching (SM): The first motor primitive achieves a desired uniform speed u_T at a given location x_T. It is thus produced by the following OC final conditions:

$$s_s(T) = x_T \quad u(T) = u_T \quad a(T) = 0. \tag{3}$$

Let us represent the solution of the OC problem for this case in a compact form as

$$\begin{aligned} s_s &= s_{s,SM}(t, x_T, u_T, w_T) \\ u &= u_{SM}(t, x_T, u_T, w_T) \\ a &= a_{SM}(t, x_T, u_T, w_T) \\ j_p &= j_{p,SM}(t, x_T, u_T, w_T). \end{aligned} \tag{4}$$

That is, the SM motor primitives are functions of time and of parameters such as the target final state u_T, x_T and the time pressure w_T. In cognitive systems terminology, u_T, x_T can be considered "perceptual goals," whereas w_T would stand for an inner motivation state.

The time horizon T that optimizes (1) is a function of u_T, x_T, and w_T, i.e.,

$$T = T_{SM}(x_T, u_T, w_T). \tag{5}$$

The actual computation of (4) and (5) may be carried out in several ways. For instance, we have developed efficient methods to solve OC problems [64], [117]–[120]; a variation of this, which exploits symbolic computation and the inherent simplicity of the forward models, is used here (e.g., see Appendix I-C). Other possibilities may be, e.g., online perception–action learning, such as used in DIPLECS.

Speed Adaptation (SA): A second type of longitudinal motor primitive is the adaptation of speed. It differs from SM in that the location at which speed u_T has to be reached is unconstrained, i.e.,

$$s_s(T) = \text{free} \quad u(T) = u_T \quad a(T) = 0. \tag{6}$$

In a similar fashion to SM, we may conceptually think that SA motor primitives are parametric in target speed u_T and motivation w_T, obtaining equations analogous to (4) and (5), i.e.,

$$\begin{aligned} s_s &= s_{s,\mathrm{SA}}(t, u_T, w_T) \\ u &= u_{\mathrm{SA}}(t, u_T, w_T) \\ a &= a_{\mathrm{SA}}(t, u_T, w_T) \\ j_p &= j_{p,\mathrm{SA}}(t, uT, w_T) \qquad (7) \\ T &= T_{\mathrm{SA}}(u_T, w_T). \qquad (8) \end{aligned}$$

b) Lateral motor primitives: Lateral motor primitives deal with the adaptation of travel direction and lateral position.

They are generated by the following OC problem:

Minimize the cost functional below with respect to a *given* final time T

$$J_n = \int_0^T j_\Delta^2(t)\, dt \tag{9}$$

subject to:

d) The forward model, given by (A1.1) in Appendix I.

e) The initial conditions, i.e., the current state

$$s_n(0) = s_{n,0} \quad \alpha(0) = \alpha_0 \quad \Delta(0) = \Delta_0. \tag{10}$$

f) The final conditions, i.e., the motor goal. As for the longitudinal case, we have two classes of motor primitives.

It is worth noting that in (9), there is no equivalent to w_T in (1). That is why the lateral OC problem (9) is formulated in an alternative way as a fixed final time T: The time T at which the motor primitive has to be completed here plays the role of w_T.

Lateral Displacement (LD): This motor primitive involves adjusting the lateral position in the lane. This is described by the following final goals:

$$s_n(T) = s_{n,T} \quad \alpha(T) = 0 \quad \Delta(T) = \kappa_T. \tag{11}$$

That is, at the end of a movement of duration T, the lateral position must be $s_{n,T}$, the travel direction must be parallel to the lane, and the trajectory curvature must match the lane curvature.

The resulting motor primitive is parametric in $s_{n,T}$ and T (one motor goal and one motivation parameter), i.e.,

$$\begin{aligned} s_n &= s_{n,\mathrm{LD}}(t, s_{n,T}, T) \\ \alpha &= \alpha_{\mathrm{LD}}(t, s_{n,T}, T) \\ \Delta &= \Delta_{\mathrm{LD}}(t, s_{n,T}, T) \\ j_\Delta &= j_{\Delta,\mathrm{LD}}(t, s_{n,T}, T). \qquad (12) \end{aligned}$$

Lane Alignment (LA): This primitive assumes that, sooner or later, the travel direction will be realigned with the lane and that the curvature will match the lane curvature κ. This process is presumed to occur in a time T and describes the lane-following task in so far as the driver is not concerned about the lateral position. The goals for this motor primitive are

$$s_n(T) = \text{free} \quad \alpha(T) = 0 \quad \Delta(T) = \kappa_T. \tag{13}$$

The corresponding primitive may be concisely summarized as a function of one parameter only (time T to alignment). Thus

$$\begin{aligned} s_n &= s_{n,\mathrm{LA}}(t, T) \\ \alpha &= \alpha_{\mathrm{LA}}(t, T) \\ \Delta &= \Delta_{\mathrm{LA}}(t, T) \\ j_\Delta &= j_{\Delta,\mathrm{LA}}(t, T). \qquad (14) \end{aligned}$$

Summing up, we have defined four motor primitives: one that achieves a specified speed at a specified location, another that adapts speed, a third that reaches a target lateral position, and a final one that realigns the travel direction to the lane. These form the bottom layer of the ECOM architecture in Fig. 4.

Of course, other primitives are possible, but these are sufficient for the current co-driver implementation.

4) Second Layer—Simple Trajectories Dealing With Obstacles or Lanes: The second behavioral layer in Fig. 4 combines the given motor units to achieve simple maneuvers that individually deal with a single obstacle, lane, or road feature (curve or landmark) at a time.

a) Obstacles: To deal with obstacles, a *predictive model of obstacle motion* is first needed. One approach would be to carry out inference of the observed vehicle intentions the same way that we carry out inference of *host* vehicle intentions, namely, reusing the framework we are developing.

However, although a fascinating research possibility, we opted not to use this approach here for a number of practical reasons: the speed and direction of travel of other vehicles is known with less accuracy than one's own, acceleration measurement tends to be unreliable, other driver controls are not directly observable, and a view of the road network from the host vehicle perspective is not easily available. These limitations could of course be overcome in future cooperative systems applications.

Follow Object (FO): The purpose of this maneuver is to approach a preceding vehicle, as in Fig. 1 using maneuver a, producing a desired time headway gap t_h.

The simplified obstacle longitudinal motion model assumes that longitudinal velocity v_o (i.e., the obstacle velocity projected onto lane direction) is fairly constant. To deal with accelerating obstacles, we rely on the continuous updating of motor plans in receding-horizon iterations. In Section IV, we discuss the limitations of this simplification.

The FollowObject maneuver is thus a perception–action map, which takes as input the object, the desired time headway, and the time pressure parameter w_T and returns an SM primitive

$$\text{FollowObject} : (object, t_h, w_T) \rightarrow SM(x_T, u_T, w_T). \tag{15}$$

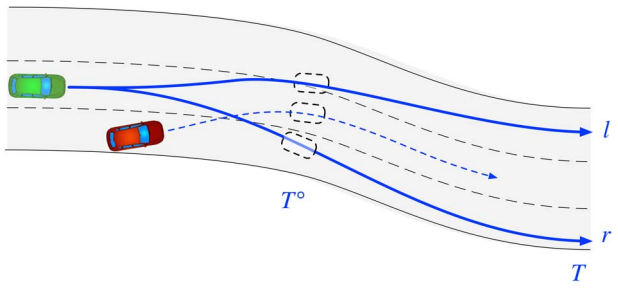

Fig. 5. Evasive maneuvers.

This means computing the target point x_T and velocity u_T that correspond to following the object as required, i.e.,

$$\begin{aligned} u_T &= v_o \\ x_T &= s_o + v_o T - v_o t_h - l_o \end{aligned} \tag{16}$$

where l_o is a longitudinal clearance that accounts for the lengths of the host vehicle and obstacle plus any extra desired clearance, $v_o t_h$ is the aimed-at time headway gap, s_o is the initial distance of the object, and T is the maneuver duration, which is obtained by solving (16) together with (5).

The FollowObject function thus instantiates an SM primitive. In Fig. 4, arrows between two levels indicate this form of input/output relationship.

The current value of the longitudinal control, i.e.,

$$j_{p,0} = j_{p,SM}(0, x_T, u_T, w_T) \tag{17}$$

is here of particular significance, because it indicates *how the co-driver ought to drive now* to follow the object, which can be directly compared with the longitudinal control that the human driver employs.

Note that the followed object does not need to be in the host vehicle's lane for this function to apply. If it is traveling in a parallel lane, including the case where it is behind the host car, then this function may be used to compute maneuvers that, for example, open a gap before a lane change may be executed.

Clear Object (CO): The purpose of this maneuver is to clear a frontal object on either side of the host vehicle (see Fig. 5).

As indicated, understanding the directional intentions of the object vehicle would ideally require knowing the road network to find which lane the obstacle might be following. Since, in the present version of the system, we only know the geometry of our own road/lane, what we can do is to assess whether the object is moving in our own road or whether it is moving *across* the road, in which case our understanding of its intentions will be correspondingly degraded.

If the object were moving in our road, its lateral movement would follow a model similar to (14), i.e., the object would sooner or later realign with the lane. Since we cannot measure the curvature of the object trajectory directly, we simplify the problem by setting $\Delta_0 = 0$ in (10), and $\kappa(.) = 0$ in (A1.1). With these simplifications, the OC problem given by (9), (10), (A1.1), (13) can be analytically solved, yielding the approximate predictive model for object lateral motion employed here, i.e.,

$$s_n = s_{n,0} + v_n t \left[1 - \left(\frac{t}{T^*} \right)^2 + \frac{1}{2} \left(\frac{t}{T^*} \right)^3 \right]. \tag{18}$$

Note that the model contains a parameter T^*, which stands for how long the object maneuver will last: in essence, a kind of intentional assessment. At this point, we do not try to estimate T^* but use the heuristically derived figure $T^* \sim 2.5$ s (see also the following section and Section IV).

The maximum LD of the object will be achieved at $t = T^*$

$$s_{n,\max} = s_{n,0} + v_n \frac{T^*}{2}. \tag{19}$$

If this position falls within one lane of the current object lane, then model (18) is confirmed (i.e., we assume that the object is following our road, possibly changing one lane only). If not, the object is considered to be crossing our road. In this case, its transverse motion is taken to be uniform, i.e.,

$$s_n = s_{n,0} + v_n t. \tag{20}$$

With an object predictive model (in our case, the simple equations 16-first, 18, 20), we can now compute evasive maneuvers, as Fig. 5 shows. The dark vehicle is the obstacle, and the dashed trajectory is its predicted motion. Even if we had a more sophisticated obstacle intention prediction, the process hereafter would be the same: first compute the encounter time T° by combining the longitudinal motion models; then produce an LD primitive (i.e., parameters $s_{n,T}$ and T) such that a specified clearance c_0 is obtained at T°.

The ClearObject function returns two LD primitives, i.e., one for clearing on the left (l) and another for clearing on the right (r). Thus

$$\text{ClearObject} : (object, c_0) \rightarrow LD(s_{n,T}, T). \tag{21}$$

The given format implies that the second layer function "ClearObject" produces the parameters $s_{n,T}$ and T of the first layer "LD" motor primitive (thus subsuming it) that clears the specified *object* at the specified distance c_0, which necessarily accounts for the width of the two vehicles plus any desired clearance. The sign of c_0 may be conveniently used to specify whether the clearing occurs to the right or to the left.

The given ClearObject behavior is simplified: First, there is only one hypothesis for T; second, there is also one hypothesis only for the longitudinal control used during the evasive maneuver, which is FF (below) with a plausible value for w_T. A discussion of this simplification is given in Section IV.

b) Lanes:

Free Flow (FF): This maneuver produces an SA primitive by guessing a target speed u_T. This is achieved by assuming a plausible value for T and solving (8) for u_T, i.e.,

$$\text{FreeFlow} : (w_T, T) \rightarrow SA(u_T, w_T). \tag{22}$$

Strictly speaking, FreeFlow should be a function of two parameters, with T dictating how long the acceleration lasts.

However, since T weakly influences the first part of the maneuver, the co-driver always generates only one hypothesis for T (which is 5 s) and relies on receding-horizon updates to refine the estimate of the latter part of the maneuver.

Lane Follow (LF): This is a wrapper for the LA/LD motor primitives. It takes as input a desired lateral position in a specified lane (in lane units) and the maneuver time T and returns an LD or an LA primitive (the latter if the final lateral position is free), i.e.,

$$\text{LaneFollow} : (lane, position, T) \rightarrow LD(s_n, T). \tag{23}$$

LandMark/SpeedLimit (LM): Landmarks are used to represent speed limits at specified locations such as at the beginning of a road section with a posted speed limit. The Landmark function takes the speed limit and position and returns an SM primitive (making only one hypothesis for w_T), i.e.,

$$\text{LandMark} : (speed\ limit, position) \rightarrow SM(x_T, u_T, w_T). \tag{24}$$

Curve (CU): This returns an SM primitive that approaches a curve with the correct speed. We use curvature data from ADAS digital maps to compute the appropriate location. The speed is derived from the two-thirds power law [98], with two hypotheses representing two different percentiles of driver lateral acceleration. Only one hypothesis is made for w_T, i.e.,

$$\text{Curve} : (curve, driver\ percentile) \rightarrow SM(x_T, u_T, w_T). \tag{25}$$

5) Third Layer—Navigation: So far, the functions of the second layer may be regarded as operators that translate simple goals, considered separately, into motor primitives. Except for CO, they return either a longitudinal or a lateral primitive.

The third layer is thus responsible for putting together these potential motor tasks into executable navigation plans. In other words, the third layer produces maneuvers (coupled longitudinal/lateral motor plans) that represent *higher-level* intentions, such as a, b, c, and d in Fig. 1.

It is worth noting that this layer still produces multiple maneuvers. For an autonomous system, they represent covert motor alternatives, such as in Fig. 1, from among which to choose. For a co-driver, they constitute hypotheses to be tested against the observed behavior of the driver.

The co-driver thus needs to produce a number of hypothetical motor activities spanning the space of possible intentions. To generate a complete set of hypotheses, the co-driver starts guessing what the lateral intentions of the driver might be. For a single road, with possibly multiple lanes, it thus generates an ensemble of LF motor tasks as shown in Fig. 6.

Three of these, labeled 1–3 in Fig. 6, are of type LA, with three hypotheses for the alignment time $T \in \{T_1, T_2, T_3\}$. These will serve to test whether the driver is going to simply realign with the lane without any particular care for the exact lateral position in it. In our implementation, the times T_1, T_2, T_3 are set at 3, 1.5, and 1 s, respectively, with the first two turning out to be the most frequent matches.

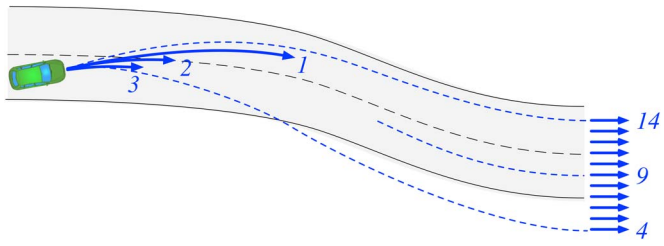

Fig. 6. Hypotheses for the lateral intentions of the human driver.

In addition, the co-driver makes 11 hypotheses of type LD, labeled 4–14 (12), in which the final lateral position $s_{n,T}$ spans three lanes, from the adjacent right lane to the left lane in steps of 0.25 lane widths (see Fig. 6). Note that the hypothesis labeled 9, corresponding to $s_{n,T} = 0$, which represents the intention to return to the *center* of the lane. Hypotheses 8 and 10 are, respectively, 0.25 lanes off-center, which approximate the intention to move near to one edge of the lane. Hypotheses 7 and 11 represent the intention to go over the lane divider (possibly as the beginning of a lane change), and the remaining hypotheses are complete lane changes. Note also that, while in Fig. 6 there is no right lane at all, hypotheses 4–7 are nonetheless generated, which represent "running out" of the lane. The reason for this excess hypothesis generation is also to test for possibly incorrect driver actions.

In the case of road forks, such as in Fig. 1, another array of hypotheses similar to those mentioned would be needed to accommodate the bifurcation. This has not, as yet, been implemented within the system.

The next step is the association of each lateral motor plan with one (or more) longitudinal plan.

Obstacles are first considered: for each, the FollowObject and ClearObject maneuvers are computed [with the same T in (21) as in (12)]. Then:

- If the ith lateral maneuver (see Fig. 6) clears all the obstacles, then it is associated to a FreeFlow longitudinal primitive representing the intention of traveling along a noncolliding path. For simplicity, we make only one hypothesis for the FF parameter, i.e., w_T (a value that represents "calm" driving), because it is not as important to understand how fast the driver wishes to drive in this case.
- If the ith lateral maneuver (see Fig. 6) falls within the $l-r$ interval of one or more objects, then the FollowObject maneuver for the most demanding object is selected. In this case, we make two hypotheses for the time headway t_h, which are 1.1 and 0.6 s.

Curves are then considered: For every curve, the CU primitive is computed, and the most demanding one retained. This is associated with all the trajectories sharing the same road path, e.g., in Fig. 1, a, c, and d share the most demanding curve primitive of the main road path, and b of the bifurcation path.

Finally, landmarks and speed limits are considered the same way as for curves.

After the given process, we end up with a list of maneuvers with both lateral and longitudinal control of two types: the first are trajectories that do not collide with obstacles, which are

associated to FreeFlow longitudinal control; the second are trajectories that might collide with an object, which are associated with two hypotheses for longitudinal control, corresponding to *tight* and *very tight* time headway. In addition, every maneuver is also associated with an alternative curve and a landmark longitudinal primitive. The reason for keeping the longitudinal primitives separate, instead of taking the most critical one, is the same as for the out-of-lane hypotheses in Fig. 6. That is, to test for mistakes, such as being able to understand that a driver may be approaching the front vehicle correctly but not a curve within the same road (or perhaps the driver has ignored the speed limits).

6) Fourth Layer—Strategy: The topmost layer is where inference of intentions is completed and interactions are born. For a correct inference of intentions, the hypotheses generated at layer 3 must thus be tested. We use a saliency-based approach, which considers both the "distance" between the hypothesis and the driver behavior and also the "plausibility" of the hypothesis itself. For the ith candidate maneuver, a penalty is therefore computed as

$$J_i = w_\Delta \left\| j_\Delta - j_\Delta^* \right\|^2 + w_p \left\| j_p - j_p^* \right\|^2 + w_n J_n. \qquad (26)$$

The first term is the square of a proper distance function between the co-driver steering control $j_\Delta(t)$ and driver control $j_\Delta^*(t)$ with weight w_Δ. The second term is the distance between the longitudinal controls, $j_p(t)$ versus $j_p^*(t)$ with weight w_p. These two together measure the "distance" between the driver and the ith co-driver hypothesis.

The third term is the steering cost of the maneuver as defined by (9). Adding this term means that maneuvers with higher steering costs are considered less plausible. Thus, for instance, a maneuver that requires less steering activity such as going straighter would be preferred to one that steers more, for the same distance to the driver behavior. However, we have not included a similar term for the longitudinal control (1).

The computation of the distance between driver and co-driver maneuvers implies a time window for the comparison, which determines a tradeoff between accuracy and delay of inferred intentions (longer observations may be more accurate but cause more delay).

Our implementation aims at quickly discriminating among the tactical maneuvers of layer 3 and, thus, uses nearly instantaneous comparison windows: For every hypothesis, the current values of the predicted longitudinal and lateral controls, i.e., $j_\Delta(0)$ and $j_p(0)$, are respectively compared with a 200-ms first-order filtered value of the steering wheel rate $\bar{j}_\Delta^*$ and with a Kalman estimation of the longitudinal jerk $\bar{j}_p^*$, i.e.,

$$J_i = w_\Delta f^- \left(j_\Delta(0) - \bar{j}_\Delta^*\right)^2 + w_p \left[j_p(0) - \bar{j}_p^*\right]^2 + \frac{1}{T} J_n. \quad (27)$$

The function f^- is the negative part, returning zero if the co-driver is faster than the human driver.

Let us, for convenience, introduce the representation in Fig. 7, which shows the control output space: the steering wheel rate j_Δ in abscissa and the longitudinal jerk j_p in ordinate. A maneuver is represented here by a curve parameterized by time, such as in the last terms of (12) and (7).

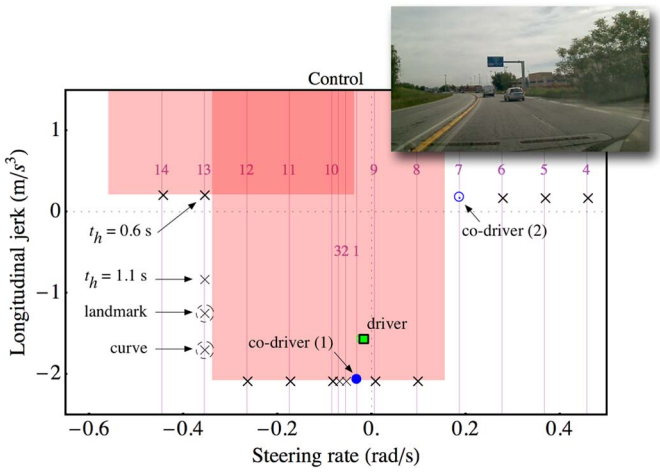

Fig. 7. Chart representing the projection of the system states onto the motor output space.

Conceptually, this chart may be regarded as a projection of the internal state of the cognitive systems onto the motor output space. This is inspired by embodied cognition, in which perception–action links imply that internal perceptual states of the system may be represented in terms of their motor output or a common code [121]–[123].

In the chart, the vertical lines labeled 1–14 represent the lateral control $j_\Delta(0)$ of each lateral motor primitive generated at layer 3, e.g., those in Fig. 6. The two overlapping rectangles stand for two vehicles, which can be seen in the inset. The tallest rectangle is the nearer car. Rectangles are bounded by the left and right ClearObject maneuvers and by the FollowObject maneuver at the bottom side.

The cross markers $(\times)$ are the maneuvers produced at layer 3. Maneuvers 4–7 clear both objects on the right and are associated with FF longitudinal primitives, whereas the others are associated with the FO primitives. Since there are two hypotheses for time headway ($t_h = 1.1$ s and $t_h = 0.6$ s), there are indeed two FO primitives for each trajectory. For clarity, we show only one ($t_h = 0.6$ s), except for the example trajectory 13, in which the second one is shown in light gray ($t_h = 1.1$ s).

In the case given here, there is no critical curve and no landmark in front of the vehicle. If there were, additional maneuvers would be generated for every trajectory such as those shown in dotted circles.

The filled and empty circles, respectively, trajectories 1 and 7, are the matching co-driver maneuvers.

The filled circle "co-driver (1)" corresponds to criterion (27) with $w_p = 0$. By weighting only the lateral control, this maneuver represents the intentional trajectory of the driver. Conversely, maneuver "co-driver (2)" uses a large weight w_p and typically preserves the longitudinal speed, producing an evasive maneuver.

The reason for selecting two maneuvers here is related to the specific use of the co-driver in the CRF application (see below). Other usage might instead require the identification of one maneuver, which can be achieved via a uniqueness-weighting scheme.

E. CRF Co-Driver Use and Human–Machine Interactions

In the CRF implementation, the co-driver is used as a tutor, exploiting the two given alternative maneuvers.

For maneuver "(1)," the co-driver determines whether the longitudinal control j_{p} corresponds to a correct maneuver or, if not, which longitudinal control should be used. For example, suppose that the "co-driver (1)" maneuver were trajectory 13 with $t_h = 0.6$ s. In this case, the correct maneuver should be at least 13 with $t_h = 1.1$ s (not considering landmarks or curves that might be present), and the co-driver would also then implicitly know how to rectify the driver's behavior. This information is thus used by the HMI of the continuous-support function, which is inactive when the driver's maneuvering is correct but produces a feedback with the required correction (and the cause of activation) otherwise.

The co-driver also establishes whether the lateral control is correct, and this information is also used by the HMI for lateral feedback. For instance, trajectory 13 corresponds to a prohibited lane and would produce lateral feedback if chosen (the same happens if the driver selects a lane that is occupied by a lateral/rear vehicle).

The evasive maneuver "co-driver (2)" is an alternative option for rectifying driver mistakes, which acts on the lateral control instead. By way of example, in Fig. 7, the co-driver "sees" that it is possible to change lane to the right to preserve longitudinal speed. Within the CRF implementation, evasive maneuvers are used to a limited extent in two cases: 1) If the evasive maneuver is within the same lane of the primary maneuver, which happens for example if an obstacle occupies only part of the lane, such as a vehicle on a nearby lane but very close to or slightly inside our lane, in which case this maneuver is selected for generating feedback in place of the original maneuver. Thus, the driver will not receive longitudinal feedback but rather a lateral feedback, e.g., because he/she must open a greater clearance with respect to a vehicle very close to or slightly inside the lane. It is worth noting how "adaptive lane keeping" is thus produced from more basic principles that reproduce human driving. The second case occurs 2) when "co-driver (1)" is a correct lane change but with short front time headway, and "co-driver (2)" is FF in the current lane. In this case "co-driver (2)" is used for feedback, indicating to the driver that he/she should better remain in the current lane.

IV. Experiment and Results

The system has been tested with ordinary drivers on public roads. The test route was a 53-km loop from CRF headquarters in Orbassano (Turin, Italy) to Pinerolo, Piossasco and back, which included urban arterials, extra urban roads, motorways, roundabouts, ramps, and intersections. The test vehicle is equipped with sensors to detect obstacles and lane geometry, on board maps with road geometry, GPS receiver for positioning on the map, and human–machine interface (HMI) devices to generate warnings and haptic feedbacks for the driver based on output from co-driver implementation running at a 10-Hz update rate. In the test, 24 subjects drove twice, with active or inactive HMI in random order. A total of 35 hours of logs have been collected, including sensor data, co-driver output, and images from a front camera. More details may be found in [98].

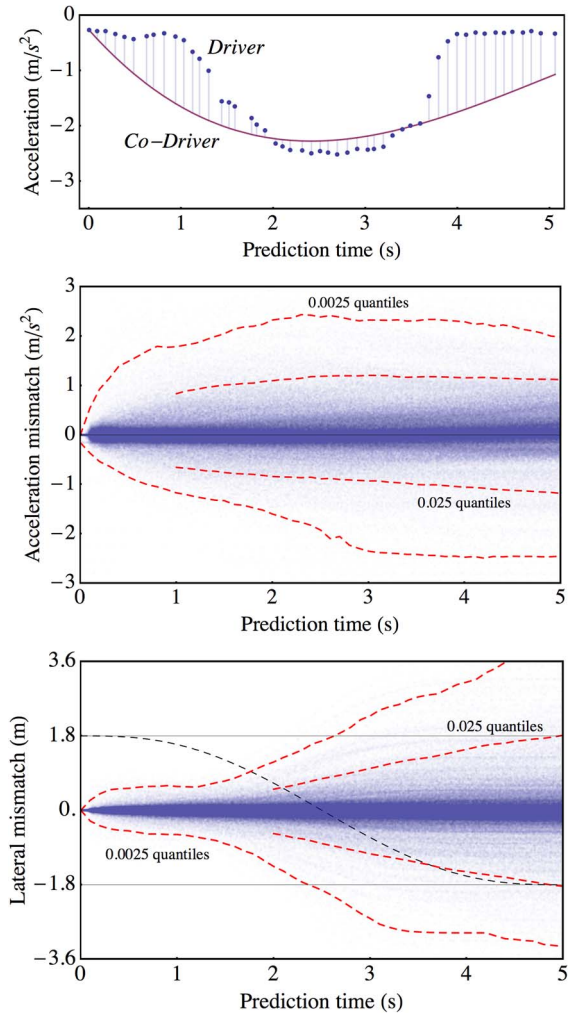

Fig. 8. (Top) Difference in longitudinal acceleration between the two agents. (Center) Distribution of acceleration difference. (Bottom) Distribution of lateral position difference.

This section focuses on the results that compare the covert driving of the co-driver to the real driving of the driver.

A first indicator, to assess whether the two agents agree, are the distance metrics (26) or (27). However, when the two agents disagree, to assess the reason, it is necessary to manually inspect the recordings. Reasons for mismatch may be 1) poorly optimized co-driver (frequent during development), 2) perception noise, 3) driver error, and 4) simple difference of "opinion" between the two agents (see below).

Fig. 8(a) shows an example situation, which happened 1.1 s before the event depicted in Fig. 7, when, for the first time, the co-driver detected a risk for maneuver 1.

Fig. 8(a) compares the longitudinal acceleration of the two agents: The driver did nothing for approximately the next second (in the meantime, a warning was issued). Then, beginning at about 1.1 s, the driver used the same longitudinal acceleration the co-driver planned 1 s earlier. Later, after ∼3.7 s, the driver departs again from the (current) co-driver plan. In this example, the difference between the two agents may be attributed to a delayed reaction of the human driver and (after 3.7 s) to sudden

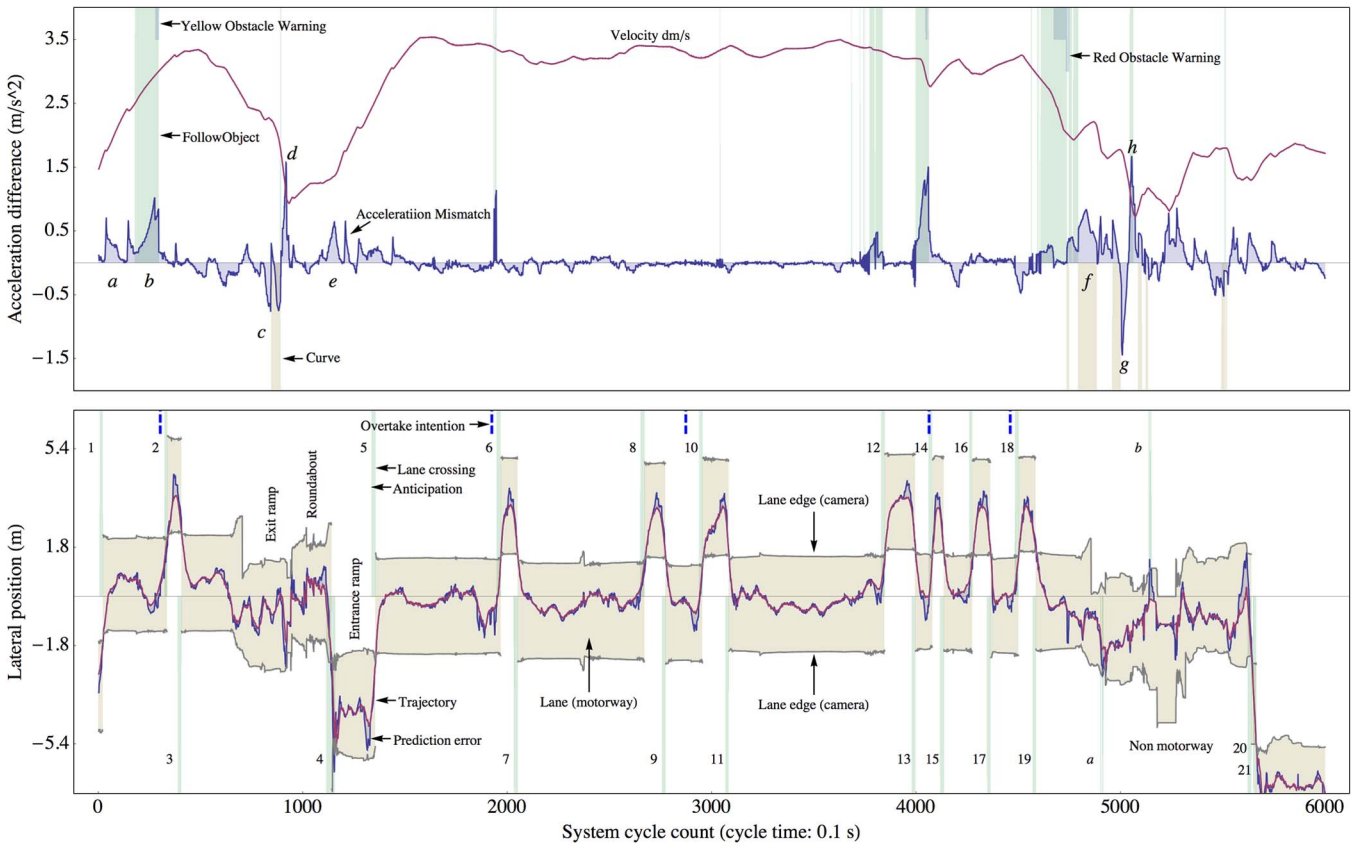

Fig. 9. Comparison of driver and co-driver on a 10-min course. (Top) Longitudinal dynamics (see text). (Bottom) Lateral dynamics.

brake release, accepting a slightly short time headway (0.9 s) for a while.

If the difference between the two agents (driver minus co-driver acceleration) is plotted for all frames together, a distribution similar to that in Fig. 8(b) is obtained. Similarly, for lateral control, the difference between the lateral positions (co-driver minus driver) yields the distribution in Fig. 8(c).

Before commenting further, let us introduce Fig. 9, which provides a different interpretation, looking at data during a course sample of 10 min.

Fig. 9(a) thus plots the average difference of the two agents' acceleration in the 5-s prediction window [i.e., the mean of the differences shown in Fig. 8(a)].

In a, d, e, and similar situations later, the human driver employs relatively high accelerations in low gears. The co-driver does not try to discover exactly how fast the human would like to drive because it is not important: these are FreeFlow states.

Another reason for mismatch occurs in situations similar to b. This case corresponds to a FollowObject state (15), which happens when the longitudinal control is limited by obstacles ahead. FO states are marked with vertical bands (light green in the online version of the paper). In the FollowObject state (such as in b) a typical pattern is often observed: As the vehicle ahead gets closer, the difference between co-driver acceleration plans and the real driver execution increases (the driver going faster) until the co-driver state switches to short (between 1.1 and 0.6 s) and very short (below 0.6 s) time headway. Note that this is not the current time headway but the time headway *goal* used in (15), which may be reached at the end of the motor unit, i.e., the intention of the driver. A yellow or red warning is issued by the HMI, marked with gray dents in the bands, for short (less than 1.1 s) or very short (less than 0.6 s) intentional time headways.

These two reasons together explain the upper part of the distribution in Fig. 8(b), with the 0.0025 quantiles curve corresponding to the largest differences occurring in a dangerous situation. Thus, the quantiles curve peaks at approximately 2–3 s in the future (related to delayed reaction of the driver).

Mismatches of the opposite sign (the driver using less acceleration than the co-driver) primarily occur before curves, such as c and g, which are, however, at a roundabout entrance. The driver, approaching a 'yield' sign, reduces speed more than simply required by the curve (and sometimes even stops), presumably for visibility reasons that are not considered by the co-driver. This discrepancy is not dangerous. The condition in f is instead one curve where the driver goes faster. However, not faster enough to trigger a dangerous curve state.

The "slowness" of the driver explains the lower part in Fig. 8(b).

Overall, the two agents disagree for three reasons, of which one is incorrect driver behavior, the other two being concretely different choices, in which one of the two opts for going slower.

The root mean square of the acceleration mismatch is 0.25 m/s^2, which is approximately the darker strip in Fig. 8(b).

Fig. 9(b) deals with the lateral dynamics. A partly rectified representation is used, which shows the lane changes. Both trajectory and prediction error are plotted (respectively violet and blue in the online version). The lane edges, as seen from the lane recognition camera, are shown, and the lane itself is

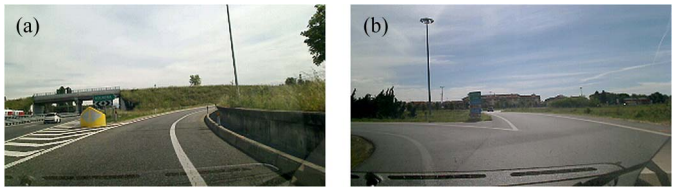

Fig. 10. Complex geometry at false-alarm points.

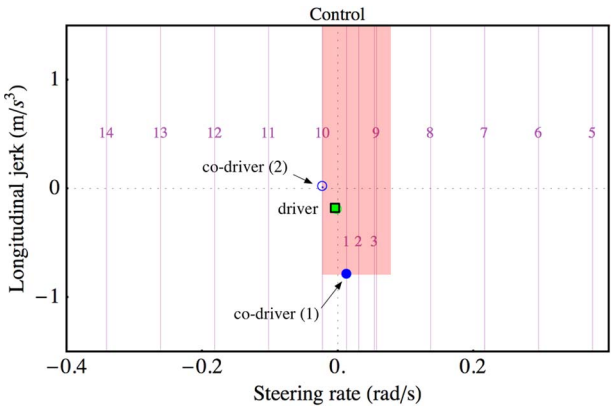

Fig. 11. Detection of the intention to overtake (the camera view for this is given by the top-right frame in Fig. 12).

shaded. Non-motorway sections, including ramps and roundabouts, exhibit a quite complex geometry. Note how close the driver passes to edges during transitions (e.g., taking the first exit ramp at cycle ∼700). The numbered light green bands stand for the lane changes. The interval between when the LD motor primitive predicts the lane crossing and the actual crossing of the lane is shaded. There are 21 changes correctly predicted, with anticipation ranging from 1.1 to 2.4 s (median 1.6 s).

There are two false crossing predictions, labeled a and b, that happen in the non-motorway section when the trajectory passes close to edges. Fig. 10 shows the camera view to demonstrate how demanding this situation actually is. Despite the false prediction, the absolute value of the lateral prediction error is limited (a fraction of the vehicle width). Non-motorway segments are characterized by often-irregular lane geometry, with splitting and merging lanes, often with missing marking traits [see Fig. 10(b)], or else the camera failing to recognize them.

Fig. 8(c) shows that 0.0025 quantile curves, i.e., 99.5% of the LD motor primitives, depart from the real trajectory for less than one quarter of a lane in 2 s, less than half a lane in 2.5 s, and less than one full lane in 5 s. The points where larger deviations happen may be seen in Fig. 9 (the prediction error is plotted). They are typically at inversions of the heading angle and in complex geometries (a and b).

In Fig. 9(b), the dashed blue vertical lines before lane changes 2, 6, 10, 14, and 18, mark the point where the co-driver switches from FollowObject (second-level) behavior to ClearObject behavior. This is the point where the agent realizes that the human *intention* may be *to overtake*.

For example, Fig. 11 shows the control output space 4.1 s before lane change 18, showing how the driver is going to choose the overtake maneuver.

These events represent a different form of inference of intentions, pertaining to a *higher cognitive level*, which are detected by the switching from FollowObject to ClearObject second-level behaviors, with the intention to overtake being not yet manifested in terms of LD motor primitives.

This happens with anticipation ranging from 1.6 to 8.1 s (median 4.1 s).

Fig. 12 summarizes the situations for the five lane changes with overtaking. It shows the camera view when the overtake intention is detected (first row), when the lane crossing is predicted (center), and when it actually takes place (bottom). The last element of the first row, at the top right, is associated with Fig. 11. In case 14, the "overtake" state and the "lane crossing" state simultaneously happen, when the left lane becomes free (fourth column in Fig. 12).

A. Comparison With Other Approaches Within the Literature

A number of alternative approaches exist in the literature for prediction of intent in driving. A review is given by Doshi and Trivedi [124], and Lethaus *et al.* focused on gaze in [125].

The vast majority of methods are classifiers that learn and recognize stereotyped head or gaze patterns preceding action execution. Preattentive vision may also be important [74].

While these methods may use a variety of algorithms (e.g., hidden Markov models, neural networks of various kinds, and Bayesian networks), they belong to a single class of intention inference methods termed as "*action-to-goal*" (Csibra and Gergely [126]), which predicts the "likely outcome of ongoing activity."

Conversely, the method of this paper belongs to the "*goal-to-action*" approach, which is also defined as "teleological," which means that actions are functional to some end [126] and consequential to that end. The teleological interpretation thus moves from a plausible goal to a generation (from which the method is also termed "generative" [55]) of the expected sequence of actions, with the granularity level sufficient for comparison with observed actions. It thus *anticipates* expected actions before they actually begin (if they do not begin, a revision of the intentions is carried out) and is hence termed "predictive tracking of dynamic actions" [126].

The prediction of overtaking, for maneuvers 2, 6, 10, 14, and 18 is one example of "goal-to-action." It is obtained because the overtake maneuver is the only one that *has meaning* (see Fig. 11) within the context. It thus anticipates the appearance of the LD motor primitives by a few seconds (see Fig. 12).

An interesting comparison can be carried out with the method of McCall *et al.* [127], which shows that learning and classification of the head pose helps to predict lane changes. Simple trajectory forecasts produce discrimination power (DP) equal to 0.95 at 2.5 s before lane change (95% detection probability and 5% false-alarm rate in lane keeping). By including head movement classification, the same DP is achieved 0.5 s earlier.

For trajectory forecast, a comparison may be attempted with Fig. 8(c). This distribution potentially allows for derivation of false-alarm rates and detection probabilities. For example, for a vehicle keeping the lane at the center, the two horizontal lines at -1.8 and $+1.8$ m represent the lane edges. The forecast

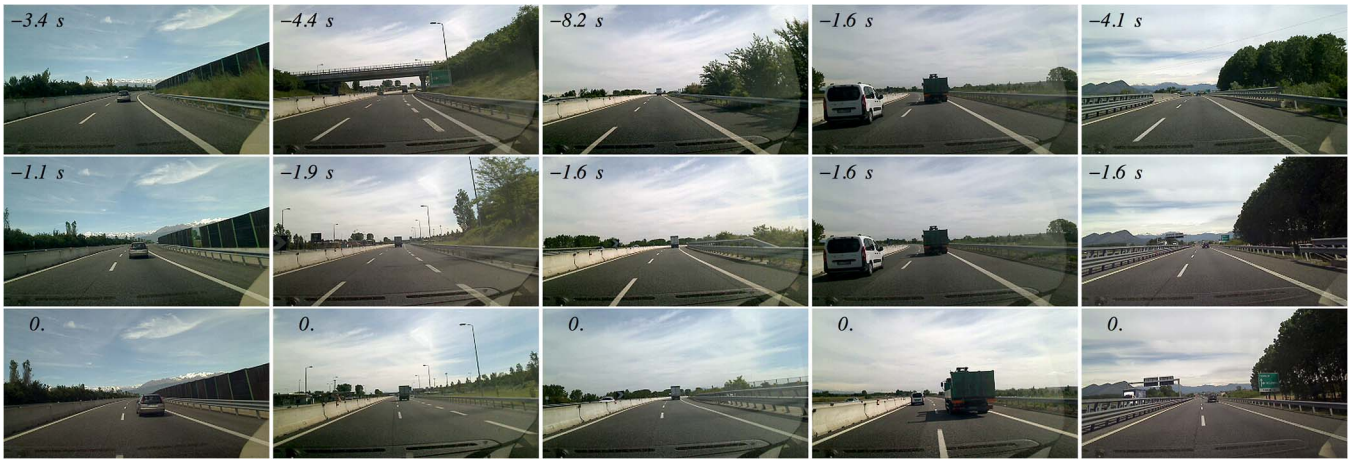

Fig. 12. Anticipation of overtake, anticipation of lane change, and actual lane change for cases 2, 6, 10, 14, and 18 (left to right). First row: overtake intention detected as second-level state transition (FollowObject to ClearObject behavior). Second row: lane change detected as motor primitive level transition (LD crossing the lane). Third row: actual lane crossing.

co-driver trajectory falls outside of the lane at 5 s with 5% probability (2.5% per side), which becomes 0.5% if the forecast is considered at 2.5 s. Conversely, for a lane-change maneuver, the left edge might look like the dashed s-shaped line (from $+1.8$ to -1.8 m). Thus, an estimation of 97.5% detection probability may be derived (as the proportion of trajectories falling above the lane edge at the end).

However, this ideal situation is not achieved because the vehicle starting position may be closer to one edge or may follow a different profile. Indeed, the two false alarms occurred within the example data set in such conditions. The situation is actually clearer for motorways than complex curved geometries due to greater quantities of perception noise and lower accuracy of the forward emulator.

McCall (and others) use a classifier to predict the probability of lane change, which is then binarized with a proper threshold choice. Different thresholds produce different couplings of detection probability and false-alarm rates, which are plotted as receiver operator characteristic (ROC) curves.

Conversely, the co-driver of this paper returns one maneuver from a discrete set of hypotheses. There is thus no equivalent of thresholding and ROC curve calculation. The performance estimated above must be considered as one point in the ROC chart, representing an upper limit. On the other hand, the reasoning leading to the estimation of performance gives an insight into the factors that affect false-alarm rates and detection probability, namely, lane geometry, initial position, maneuver profile, etc.

Thus, further comparisons would be difficult to interpret, given the different nature of the roads (narrower lanes, ramps, roundabouts, etc.) and the unknown differences in the quality of the perception system (in particular, we used a commercial lane-recognition camera with significant lag, because this was specifically designed for motorway use).

As for the higher-level cognitive intention recognition, the effect of head-pose classification (action-to-goal) can be compared with the (goal-to-action) prediction of the overtaking maneuver. The latter appears to be more anticipatory, as might be logically expected from a goal-to-action approach.

V. Discussion

A. Inference of Intentions

Perhaps the most wide-ranging conclusion concerns the nature of the inference of intentions.

We have seen that the inference of intentions is achieved within the co-driver by fitting observed behaviors onto sensory-motor hypotheses of another agent. What is essentially taking place is that the latter agent interprets the observed behavior in terms of its *own* states that would produce it. Thus, attempting to make the co-driver sensory-motor system as human-like as possible is a precondition for its effectiveness, and studying human motor strategies is an important related research field (as it is in human–robot peer interactions).

One related point is that the hypotheses of the interpreting agent may be limited in number or may not be complete, thus missing or approximating the real case. This may happen even if the two agent's sensory-motor systems are very similar.

Approximations may arise from making a finite, limited, and discrete set of hypotheses. Behavior is thus approximated by the nearest hypothesis. However, if the discretization is made with hypotheses that are qualitatively different (e.g., taking one of two choices at a bifurcation), then this potentially helps reject noise (e.g., any activity approximately equidistant between two bifurcating roads is interpreted as either one of the two).

The reason for generating a limited set of hypotheses may also be because the dimensionality of the cognitive system states is much greater than that of the motor output space. Short-time observations of the motor output easily discriminate between subsets in state space, but there are states that project onto very similar motor outputs for a duration and would require longer observations to be distinguished (i.e., states are not equally observable). One example is the distinction between $s_{n,T}$ and T in the LD primitive, which are not easily discriminated during the short-term observations that are required for our driver assistance application. This may be partly solved by taking a "plausible" assumption for one of the two, which is indeed what was done for T.

Incomplete sensory-motor systems are lacking perception–action loops for some layers of the ECOM architecture. Fortunately, higher-level behaviors are composed of simpler lower-level units, and thus, a system missing one behavior such that it may not be able to model the intentions at that level may instead be able to understand the single phases in which it is decomposed. For example, in our model, there is no built-in behavior for navigating around an object. However, this functionality may be obtained with a sequence of lower-level behaviors such as 1) clear object or change lane, 2) free flow until the object is passed, and 3) lane change back again. As a consequence, while the co-driver as implemented is literally unable to model overtaking maneuvers, it yet understands the single phases of the maneuver as they occur.

Fortunately, interpreting the situation in terms of lower-level behaviors in this way still produces the correct interactions (for example, if one driver begins the cut-in maneuver too early after an overtake, the advice to "keep clear" is produced even if the co-driver was not aware that it was the final part of a composite maneuver).

Hence, the system is, to a large extent, robust against the absence of high-level motor plans if these can be decomposed into simpler units, of which the system is instead aware.

Despite this robustness, the question of scalability of the system is important. In this respect, the proposed behavioral architecture permits easy extension and scalability. It would not be difficult, for instance, to design an "overtaking" maneuver, which, just like the examples given in Section III, returns a specific sequence of motor units when given a set of perceptual goals. If such sequences can be associated with a compressed perceptual parameter space [128], [129], then strict cognitive bootstrapping is achieved, with spontaneous abstraction of the perception–action hierarchy.

The topic of how to make the system capable of self-extension is thus important and indeed central in artificial cognitive studies. An interesting and relatively little-studied possibility here would be using the forward models to retrospectively rehearse hypothetical situations (i.e., "rethinking" past experiences).

B. Behaviors From Basic Principles

We noted before that our system's "adaptive lane keeping" originated from basic principles. This is not the only such case. For instance, a system that works by producing human-like behaviors is very likely to give rise to complex behaviors that have not been explicitly programmed.

We have observed some of these, the most salient being, perhaps, the case depicted in Fig. 7. The car obstacle remains in the right lane, at the very beginning of a change of lane. Nonetheless, the co-driver predicts its own and other road users' behavior and comes to the conclusion that the car will block in-lane maneuvers, requires braking, with the only available alternative being changing to the right-hand lane. In subjective human evaluation, the warning produced by the system was indeed appreciated, being both appropriate and anticipated, giving the impression that the system "understood" the road situation and was able to correctly anticipate outcomes.

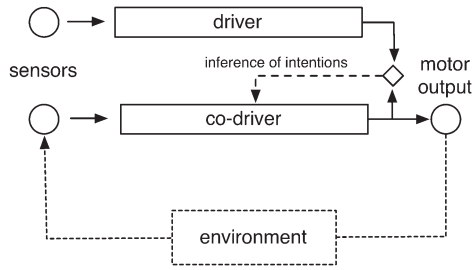

Fig. 13. Architecture of the co-driver for the H-metaphor.

C. Major Limitation

The system implemented suffers a number of limitations, the most important being noise and inaccuracy of the sensorial system. For example, a small error in the measurement of the lateral speed of other vehicle has the potential to cause the system to presume that the other driver is willing to change lane, causing false alarms. We observed several such false alarms in 35 h of user tests.

Another limitation comes from incompleteness of the sensorial data. For example, knowing only the geometry of the host vehicle lane, and not that of the intersection lanes, caused some false alarms in which vehicles moving to other lanes could not be accurately predicted. A typical example is the entrance of a roundabout where the vehicle leaving the roundabout in the opposite lane may look like it is intersecting our lane. We observed one such false alarm in the user tests.

The last set of limitations is a direct consequence of the incompleteness and simplification of the sensory-motor system of the co-driver. For example, the FO maneuver presumes that the antagonist vehicle is moving with only little longitudinal acceleration. If this is the case, then the small errors due to the model assumptions (16) are corrected by the receding-horizon scheme. However, it happened in the technical tests (prior to the user tests) that the other vehicle performed a hard brake. The co-driver thus continuously underestimated the deceleration needed by the follow maneuver, resulting in a late warning (however, this would also happen to humans if brake lights were absent). A better tracking of objects combined with improved motor primitives could of course fix this limitation.

VI. Conclusion and Impacts

A. Impact of Co-Driver Technology

In the example given in Section III, the co-driver is used in a limited form to produce a comprehensive preventive safety system capable of giving information and warnings only.

However, co-drivers are potentially suited to more sophisticated applications. Let us consider the application scheme given in Fig. 13, where driver and co-driver sensory-motor activities run in parallel, up to the point at which they are compared. Thereafter, it is up the co-driver to control the vehicle; however, this must be in accordance with the driver's intentions. Driving a system like this would resemble horse riding (the horse "reads" the rider and complies with his/her intentions).

This can be achieved by extending layer III.6, implementing the desired interactions after the inference of intentions.

As in the rider–horse metaphor, a system like this could be designed to complete maneuvers of which it had had hints from the driver, just like the ESP work for chassis control, albeit at a much higher cognitive level.

If necessary, the driver could "loosen" control (just like a rider loosens the reins) and let the system autonomously navigate, or "tighten" control (just as a rider tightens the reins) and reclaim authority. If necessary, the system may be programmed to completely take over from the driver in certain conditions.

In all cases, the driven vehicle should appear to be driven by a human, thus being interpretable to other human road users.

The co-driver is thus the enabling technology for implementing the speculative interactions proposed in [3]–[7].

The co-driver could have capabilities other than improving human–vehicle interactions. In cooperative systems, co-drivers could be used in a number of different ways, but principally by exchanging intentions between co-driver-equipped vehicles. This would improve much of the motor imagery, particularly functions FollowObject, ClearObject, and so on. In a less direct way, a co-driver could also be used to observe other road users and infer their intention, e.g., in a way similar to (18) and (19) but potentially much more effective overall.

Finally, the architecture in Fig. 4, if combined with learning abilities (such as those demonstrated in DIPLECS), could be used to rehearse critical situations, rare events, etc. The system could use its emulation capacity (in a way similar to human rehearsing of possible experiences) to discover and learn higher-level behaviors that might prove more effective.

This enables the co-driver to become an expert driver without directly needing training examples from expert humans. If combined with cooperative systems, this ability may also enable the co-driver to analyze accident scenarios that rarely happen, thus improving their overall motor strategy.

B. Final Remarks

In this position paper, we have attempted to set out a viable roadmap for producing the co-driver enabling technology, making significant use of recent developments in cognitive systems.

We have set out an example of a system that was developed as part of a European Integrated Project, showing that at least some of the basic co-driver functionality can be readily achieved.

Other achievements will need further research at the intersection between cognitive sciences and intelligent vehicles.

APPENDIX I

A. Lateral Forward Model

For the lateral forward model, we adopt the steady-state cornering equations of a classical bicycle model and make them into a quasi-static model.

We may obtain the equations either by following a classical steady-state cornering approach, such as in [100, Ch. 3.3], or by neglecting the frequency dependence (i.e., by retaining only the static gain) in the transfer functions of the vehicle lateral response such as in [100, Ch. 3.4.2].

The resulting equations are projected in a curvilinear coordinate system following the lane geometry, as was used in [130, Sec. 3.2]. The resulting set of equations is thus

$$\begin{aligned} \dot{s}_n &= u\,\mathrm{Sin}(\alpha) \\ \dot{\alpha} &= -\frac{\kappa(s_s)}{1-s_n\kappa(s_s)}u\,\mathrm{Cos}(\alpha)+u\Delta \\ \dot{\Delta} &= \frac{1}{k_1+k_2u^2}j_\Delta. \end{aligned} \tag{A1.1}$$

There are three state variables, namely, Δ, the curvature of current trajectory; α, the angle between forward velocity and the lane direction in the current position; and s_n, the curvilinear ordinate.

The lateral control input is j_Δ, which is the steering rate (and which is also proportional to the lateral jerk).

As is usual, when dealing with split lateral/longitudinal control (which is the case here), the vehicle speed u is considered constant in (A1.1), and consequently, the curvilinear abscissa s_n is travel speed times the time t.

The equations in (A1.1), rather than accurately modeling the lateral vehicle dynamics, aim at modeling how the human driver understands the lateral control. The third equation says he/she understands the curvature trajectory to be proportional to the steering wheel angle, with a gain changing with the speed. The constants k_1 and k_2 describe the vehicle under steering behavior, accounting also for wheelbase and the steering wheel ratio. These have been computed from the design parameters of the vehicle and later checked against yaw rate and steering wheel angle recordings taken during the experiments. We noticed that, if ignored or wrongly set, the co-driver forward model did not match human trajectories. The third equation in (A1.1) neglects the transient lateral phenomena that happen in typically subsecond time frames (see [100, Ch. 3.4.2]), which means that the driver is modeled as not being able to afford and/or control them. This simplification is probably not completely correct; however, it is adopted here because of the resulting significant simplification of the equations. We propose to evaluate ex-post the validity of such an assumption.

The second and first equations in (A1.1) simply compute the relative orientation α and lateral displacement s_n for lanes of any given geometry, described by curvature $\kappa(s_s)$ (see [130], for further details).

B. Longitudinal Forward Model

Equations for the longitudinal dynamics are straightforward

$$\begin{aligned} \dot{s}_s &= u \\ \dot{u} &= a \\ \dot{a} &= j_p. \end{aligned} \tag{A1.2}$$

These model the human driver as controlling the longitudinal jerk, which is a nonlinear function of the gas and brake pedal rate (we assume that the driver is able to invert such nonlinarites to achieve a desired rate of change of the acceleration).

C. OC Motor Primitives

For the sake of clarity, this section gives an example of the computation of motor primitives for the SM case (4). Adaptation to other cases, i.e., (7), (12), and (14), is simple. However, for lateral primitives, preliminary linearization of (A1.1) is required to produce piecewise closed-form solutions.

We used a computer algebra system (Wolfram's Mathematica), which also eased code generation.

Thus, equations (4)—which are the solution of the OC problem (1) subject to boundary conditions (2) and (3) with plant dynamics given by (A1.2)—are obtained by means of the Calculus of Variations and Pontryagin's minimum principle. Thus

$$\begin{aligned} s_{s,\mathrm{SM}} =& \frac{-a_o T^2 - 6u_o T - 6u_T T + 12x_T}{2}\left(\frac{t}{T}\right)^5 \\ &+ \frac{3a_o T^2 + 16u_o T + 14u_T T - 30x_T}{2}\left(\frac{t}{T}\right)^4 \\ &+ \frac{-3a_o T^2 - 12u_o T - 8u_T T + 20x_T}{2}\left(\frac{t}{T}\right)^3 \\ &+ \frac{a_o}{2}t^2 + u_o t \\ j_{p,\mathrm{SM}} =& 30\frac{-a_o T^2 - 6u_o T - 6u_T T + 12x_T}{T^3}\left(\frac{t}{T}\right)^2 \\ &+ 12\frac{3a_o T^2 + 16u_o T + 14u_T T - 30x_T}{T^3}\left(\frac{t}{T}\right) \\ &+ 3\frac{-3a_o T^2 - 12u_o T - 8u_T T + 20x_T}{T^3}. \end{aligned} \quad \text{(A1.3)}$$

Equations for velocity (u) and acceleration (a) are not explicitly shown in (A1.3), because they simply are the derivatives of s_s.

Since (1) is formulated as a *free* horizon problem, T, is derived from minimization of (1) after substitution of the last of (A1.3) in it, which provides a closed-form expression for the integral, as

$$\begin{aligned} J_S =& w_T T + \frac{720(x_T)^2}{T^5} - \frac{720(u_T + u_0)x_T}{T^4} \\ &+ \frac{72a_0u_0 + 48a_0u_T}{T^2} \\ &24\frac{8(u_0)^2 + 14u_0u_T + 8(u_T)^2 - 5a_0x_T}{T^3} + \frac{9(a_0)^2}{T} \\ T =& \arg\min_T J_S. \end{aligned} \quad \text{(A1.4)}$$

Thus, T is indeed a function of w_T, and so are (4).

APPENDIX II

A. Relation With Autonomous Driving

As indicated in the introduction, autonomous driving can be regarded as one extreme point of an interaction spectrum (one definition is, for example, given in SAE standard J3016).

Compared with other agents for fully autonomous driving, the most distinctive aspect of a codriving agent lies in its ability to interact with humans in an anticipative manner, implying a range of novel scientific challenges.

As regards the societal necessity for co-drivers, it might be argued that the introduction of partial automation would constitute a key part of the roadmap aiming at full automation. However, even if full automation were available, a co-driver agent would be able to carry out mixed initiatives *in addition* to fully autonomous driving. From the user perspective, the *user experience* would be completely different, with autonomous-only vehicles resembling taxi systems and co-drivers resembling the rider–horse interaction (even when acting at the full automation level). This might, in turn, motivate the preference for co-driver systems in a large number of market segments.

In addition, considering the interaction with vulnerable road users, for example, pedestrians and cyclists, inference of intentions in both directions cannot ultimately be omitted: Pedestrians and cyclists must predict maneuvers of vehicles, and vice versa. Thus, inference of intentions based on mirroring principles, which is perhaps the major contribution of this paper, constitutes a potentially significant contribution for autonomous vehicles.

Concerning trajectory planning, while the major focus of autonomous vehicles has been on the planning of collision-free maneuvers in dynamic environments with respect to the limits of maneuverability and of the actuators, in the case of mirroring, the focus is on the planning of maneuvers *with respect to the human sensory-motor limits* (i.e., human-like maneuvers).

The adoption of the Brooks subsumptive architecture, which reuses collision-free atomic motor units, may be one way to ensure safe higher-level behaviors in both cases (indeed it was originally proposed for an autonomous robot [17]).

However, (and fortunately) humans do not use the whole maneuverability envelope of the vehicle. For example, they use a fraction of the tire friction [98], and they are also limited in rate and in reaction time. Because of this, when mirroring human driving, there are still maneuverability margins that can be exploited by an autonomous intervention. Thus, preventive safety and intervention potentially fall within the same conceptual framework of reproducing human driving, with maneuvers beyond human limits (but within maneuverability limits) used as a last resort (however, this paper has focused on the first topic only).

REFERENCES

[1] R. Bishop, "Intelligent vehicle R&D: A review and contrast of programs worldwide and emerging trends," *Ann. Telecommun.*, vol. 60, no. 3/4, pp. 228–263, Apr. 2005.

[2] J. Piao and M. McDonald, "Advanced driver assistance systems from autonomous to cooperative approach," *Transp. Rev.*, vol. 28, no. 5, pp. 659–684, 2008.

[3] T. Inagaki, "Smart collaboration between humans and machines based on mutual understanding," *Annu. Rev. Control*, vol. 32, no. 2, pp. 253–261, Dec. 2008.

[4] F. O. Flemisch *et al.*, "The H-metaphor as a guideline for vehicle automation and interaction," NASA Langley Res. Center, Hampton, VA, USA, NASA/TM-2003-212672, Dec. 2003.

[5] J. Dixon, "The design of future things (Norman D.A.; 2007) [Book Reviews]," *IEEE Technol. Soc. Mag.*, vol. 29, no. 4, pp. 14–15, 2010.

[6] A. Heide and K. Henning, "The 'cognitive car': A roadmap for research issues in the automotive sector," *Annu. Rev. Control*, vol. 30, no. 2, pp. 197–203, 2006.

[7] L. Li, D. Wen, N.-N. Zheng, and L.-C. Shen, "Cognitive cars: A new frontier for ADAS research," *IEEE Trans. Intell. Transp. Syst.*, vol. 13, no. 1, pp. 395–407, Mar. 2012.

[8] HAVEit-Highly Automated Vehicles for Intelligent Transport, [Accessed: 03-Sep-2013]. [Online]. Available: http://www.haveit-eu.org/

[9] F.-Y. Wang, "Agent-based control strategies for smart and safe vehicles," in *Proc. IEEE ICVES*, 2005, pp. 331–332.

[10] F.-Y. Wang, "Parallel control and management for intelligent transportation systems: Concepts, architectures, applications," *IEEE Trans. Intell. Transp. Syst.*, vol. 11, no. 3, pp. 630–638, Sep. 2010.

[11] M. Plöchl and J. Edelmann, "Driver models in automobile dynamics application," *Veh. Syst. Dyn.*, vol. 45, no. 7/8, pp. 699–741, 2007.

[12] C. C. Macadam, "Understanding and modeling the human driver," *Veh. Syst. Dyn.*, vol. 40, no. 1–3, pp. 101–134, Jan. 2003.

[13] J. A. Fodor, *The Language of Thought*, vol. 4. Cambridge, MA, USA: Harvard Univ. Press, 1975, ch. 3, p. 214.

[14] A. Newell and H. A. Simon, "Computer science as empirical inquiry: Symbols and search," *Commun. ACM*, vol. 19, no. 3, pp. 113–126, Mar. 1976.

[15] Z. W. Pylyshyn, *Computation and Cognition: Toward a Foundation for Cognitive Science*, vol. 88. Cambridge, MA, USA: MIT Press, 1984, ch. 1, pp. xxiii, 292.

[16] K. J. W. Craik, *The Nature of Explanation*, vol. 42. Cambridge, MA, USA: Cambridge Univ. Press, 1943, ch. 3, p. 134.

[17] R. Brooks, "A robust layered control system for a mobile robot," *IEEE J. Robot. Autom.*, vol. RA-2, no. 1, pp. 14–23, Mar. 1986.

[18] D. E. Rumelhart and J. L. McClelland, *Parallel Distributed Processing: Explorations in the Microstructure of Cognition*, vol. 1. Cambridge, MA, USA: MIT Press, 1986, ch. 1, pp. 318–362.

[19] F. J. Varela, E. Thompson, and E. Rosch, *The Embodied Mind: Cognitive Science and Human Experience*, vol. 1992. Cambridge, MA, USA: MIT Press, 1991, p. 308.

[20] E. Thelen and L. B. Smith, *A Dynamic Systems Approach to the Development of Cognition and Action*, vol. 512. Cambridge, MA, USA: MIT Press, 1994, p. 376.

[21] T. Van Gelder, "What might cognition be, if not computation?" *J. Philos.*, vol. 92, no. 7, pp. 345–381, Jul. 1995.

[22] L. Steels and R. Brooks, Eds., *The Artificial Life Route To Artificial Intelligence: Building Embodied, Situated Agents*. Hillsdale, NJ, USA: Lawrence E. Psychology Press, 1995, p. 304.

[23] R. F. Port and T. Van Gelder, *Mind as Motion*. Cambridge, MA, USA: MIT Press, 1995, pp. 195–226.

[24] I. Harvey, "Untimed and misrepresented: Connectionism and the computer metaphor," *AISB Q.*, vol. 96, pp. 20–27, 1996.

[25] A. Clark, *Being There: Putting Brain Body and World Together Again*. Cambridge, MA, USA: MIT Press, 1997, p. 269.

[26] T. Van Gelder, "The dynamical hypothesis in cognitive science," *Behav. Brain Sci.*, vol. 21, no. 5, pp. 615–628, Oct. 1998, discussion 629–665.

[27] R. Pfeifer and C. Scheier, *Understanding Intelligence*, vol. 288. Cambridge, MA, USA: MIT Press, 1999, ch. 5466, p. 697.

[28] J. A. Seitz, "The bodily basis of thought," *New Ideas Psychol.*, vol. 18, no. 1, pp. 23–40, Apr. 2000.

[29] R. Beer, "Dynamical approaches to cognitive science," *Trends Cogn. Sci.*, vol. 4, no. 3, pp. 91–99, 2000.

[30] R. Pfeifer and J. Bongard, *How the Body Shapes the Way we Think*. Cambridge, MA, USA: MIT Press, 2007, p. 394.

[31] J. Gibson, "The theory of affordances," in *The Ecological Approach To Visual Perception*. Hillsdale, NJ, USA: Lawrence Erlbaum Associates, 1986, pp. 127–143.

[32] R. A. Brooks, "Intelligence without representation," *Artif. Intell.*, vol. 47, no. 1–3, pp. 139–159, Jan. 1991.

[33] L. W. Barsalou, "Grounded cognition," *Annu. Rev. Psychol.*, vol. 59, pp. 617–645, Jan. 2008.

[34] A. Clark and J. Toribio, "Doing without representing?" *Synthese*, vol. 101, no. 3, pp. 401–431, Dec. 2006.

[35] W. Bechtel, "Representations and cognitive explanations: Assessing the dynamicist's challenge in cognitive science," *Cogn. Sci.*, vol. 22, no. 3, pp. 295–318, Jul. 1998.

[36] F. Keijzer, "Representation in dynamical and embodied cognition," *Cogn. Syst. Res.*, vol. 3, no. 3, pp. 275–288, Sep. 2002.

[37] A. Markman and E. Dietrich, "Extending the classical view of representation," *Trends Cogn. Sci.*, vol. 4, no. 12, pp. 470–475, Dec. 2000.

[38] W. M. Ramsey, *Representation Reconsidered*, vol. 24. Cambridge, U.K.: Cambridge Univ. Press, 2007, ch. 1, pp. 135–139.

[39] M. Mirolli, "Representations in Dynamical Embodied Agents Re-Analyzing a Minimally Cognitive Model Agent," *Cogn. Sci.*, vol. 36, no. 5, pp. 870–895, Jul. 2012.

[40] R. Grush, "The emulation theory of representation: Motor control, imagery, perception," *Behav. Brain Sci.*, vol. 27, no. 3, pp. 377–396, Jun. 2004, discussion 396–442.

[41] D. M. Wolpert, R. C. Miall, and M. Kawato, "Internal models in the cerebellum," *Trends Cogn. Sci.*, vol. 2, no. 9, pp. 338–47, Sep. 1998.

[42] G. Hesslow, "Conscious thought as simulation of behaviour and perception," *Trends Cogn. Sci.*, vol. 6, no. 6, pp. 242–247, Jun. 2002.

[43] J. Decety and J. Grèzes, "The power of simulation: Imagining one's own and other's behavior," *Brain Res.*, vol. 1079, no. 1, pp. 4–14, Mar. 2006.

[44] J. Munzert, B. Lorey, and K. Zentgraf, "Cognitive motor processes: The role of motor imagery in the study of motor representations," *Brain Res. Rev.*, vol. 60, no. 2, pp. 306–326, May 2009.

[45] G. Hesslow, "The current status of the simulation theory of cognition," *Brain Res.*, vol. 1428, pp. 71–9, Jan. 2012.

[46] M. Jeannerod and V. Frak, "Mental imaging of motor activity in humans," *Curr. Opin. Neurobiol.*, vol. 9, no. 6, pp. 735–739, Dec. 1999.

[47] J. Decety, "The neurophysiological basis of motor imagery," *Behav. Brain Res.*, vol. 77, no. 1/2, pp. 45–52, May 1996.

[48] M. Jeannerod, "The representing brain: Neural correlates of motor intention and imagery," *Behav. Brain Sci.*, vol. 17, no. 2, pp. 187–202, Jun. 1994.

[49] M. Lotze and U. Halsband, "Motor imagery," *J. Physiol. Paris*, vol. 99, no. 4–6, pp. 386–395, 2006.

[50] M. Jeannerod, "Neural simulation of action: A unifying mechanism for motor cognition," *NeuroImage*, vol. 14, pt. 2, no. 1, pp. S103–S109, Jul. 2001.

[51] S. Hurley, "The Shared Circuits Model (SCM): How control, mirroring, simulation can enable imitation, deliberation, mindreading," *Behav. Brain Sci.*, vol. 31, no. 1, pp. 1–22, Feb. 2008, discussion 22–58.

[52] D. M. Wolpert, K. Doya, and M. Kawato, "A unifying computational framework for motor control and social interaction," *Philos. Trans. R. Soc. Lond. B, Biol. Sci.*, vol. 358, no. 1431, pp. 593–602, Mar. 2003.

[53] D. M. Wolpert and M. Kawato, "Multiple paired forward and inverse models for motor control," *Neural Netw.*, vol. 11, no. 7/8, pp. 1317–1329, Oct. 1998.

[54] D. M. Wolpert and M. S. Landy, "Motor control is decision-making," *Curr. Opin. Neurobiol.*, vol. 22, no. 6, pp. 996–1003, Dec. 2012.

[55] Y. Demiris, "Prediction of intent in robotics and multi-agent systems," *Cogn. Process.*, vol. 8, no. 3, pp. 151–158, Sep. 2007.

[56] Y. Demiris and A. Billard, "Special issue on robot learning by observation, demonstration and imitation," *IEEE Trans. Syst., Man, Cybern. B, Cybern.*, vol. 35, no. 3, pp. 254–255, Apr. 2007.

[57] Y. Demiris and M. Johnson, "Distributed, predictive perception of actions: A biologically inspired robotics architecture for imitation and learning," *Connect. Sci.*, vol. 15, no. 4, pp. 231–243, Dec. 2003.

[58] Y. Demiris and B. Khadhouri, "Hierarchical attentive multiple models for execution and recognition of actions," *Robot. Auton. Syst.*, vol. 54, no. 5, pp. 361–369, May 2006.

[59] Y. Demiris and A. Meltzoff, "The Robot in the Crib: A Developmental Analysis of Imitation Skills in Infants and Robots," *Infant Child Dev.*, vol. 17, no. 1, pp. 43–53, Jan. 2008.

[60] M. Haruno, D. M. Wolpert, and M. Kawato, "Mosaic model for sensorimotor learning and control," *Neural Comput.*, vol. 13, no. 10, pp. 2201–2220, Oct. 2001.

[61] A. Meltzoff, "Understanding the intentions of others: Re-enactment of intended acts by 18-month-old children [References]," *Dev. Psychol.*, vol. 31, no. 5, pp. 838–850, 1995.

[62] A. N. Meltzoff, "The 'like me' framework for recognizing and becoming an intentional agent," *Acta Psychol. (Amst.)*, vol. 124, no. 1, pp. 26–43, Jan. 2007.

[63] A. Amditis *et al.*, "A holistic approach to the integration of safety applications: The INSAFES subproject within the European framework programme 6 integrating project PReVENT," *IEEE Trans. Intell. Transp. Syst.*, vol. 11, no. 3, pp. 554–566, Sep. 2010.

[64] E. Bertolazzi, F. Biral, M. Da Lio, A. Saroldi, and F. Tango, "Supporting drivers in keeping safe speed and safe distance: The SASPENCE subproject within the European framework programme 6 integrating project PReVENT," *IEEE Trans. Intell. Transp. Syst.*, vol. 11, no. 3, pp. 525–538, Sep. 2010.

[65] Dynamic Interactive Perception-action LEarning in Cognitive Systems—DIPLECS, [Accessed: 04-Sep-2013]. [Online]. Available: http://www.diplecs.eu/
[66] E. Hollnagel and D. D. Woods, "Cognitive systems engineering: New wine in new bottles," *Int. J. Human-Comput. Stud.*, vol. 51, no. 2, pp. 339–356, Aug. 1999.
[67] E. Hollnagel, "Cognition as control: A pragmatic approach to the modelling of joint cognitive systems," unpublished. Available: http://www.ida.liu.se/eriho/images/IEEE_SMC_Cognition_as_control.pdf [accessed Feb 21 2014]
[68] E. Hollnagel and D. D. Woods, *Joint Cognitive Systems*. New York, NY, USA: Taylor & Francis, 2005, pp. 113–133.
[69] G. H. Granlund, "Organization of architectures for cognitive vision systems," in *Proc. Cogn. Vis. Syst.*, 2006, vol. 3948, pp. 37–55.
[70] M. Felsberg, J. Wiklund, and G. Granlund, "Exploratory learning structures in artificial cognitive systems," *Image Vis. Comput.*, vol. 27, no. 11, pp. 1671–1687, Oct. 2009.
[71] M. Felsberg, A. Shaukat, and D. Windridge, "Online Learning in Perception-Action Systems," presented at the 11th Eur. Conf. Comput. Vis., Crete, USA, 2010. [Online]. Available: http://liu.diva-portal.org/smash/get/diva2:342948/FULLTEXT01.pdf
[72] L. Ellis, M. Felsberg, and R. Bowden, "Affordance mining: Forming perception through action," in *Proc. 10th Asian Conf. Comput. Vis.*, vol. 6495, *Lecture Notes in Computer Science*, 2011, pp. 525–538.
[73] A. Shaukat, D. Windridge, E. Hollnagel, L. Macchi, and J. Kittler, "Induction of the human perception-action hierarchy employed in junction-navigation scenarios," presented at the [poster n.26] 4th Int. Conf. CogSys, Zurich, Switzerland, 2010. [Online]. Available: http://www.cogsys2010.ethz.ch/doc/cogsys2010_proceedings/cogsys2010_0026.pdf
[74] N. Pugeault and R. Bowden, "Learning pre-attentive driving behaviour from holistic visual features," in *Proc. ECCV*, 2010, vol. 6316, pp. 154–167.
[75] A. Shaukat, D. Windridge, E. Hollnagel, L. Macchi, and J. Kittler, "Adaptive, Perception-Action-based Cognitive Modelling of Human Driving Behaviour using Control, Gaze and Signal inputs," presented at the Brain Inspired Cogn. Syst., Madrid, Spain, 2010. [Online]. Available: https://www.academia.edu/544727/Adaptive_Perception-Action-based_Cognitive_Modelling_of_Human_Driving_Behaviour_using_Control_Gaze_and_Signal_inputs
[76] D. Windridge, M. Felsberg, and A. Shaukat, "A framework for hierarchical perception-action learning utilizing fuzzy reasoning," *IEEE Trans. Syst., Man, Cybern. B, Cybern.*, vol. 43, no. 1, pp. 155–169, Feb. 2012.
[77] D. Windridge, A. Shaukat, and E. Hollnagel, "Characterizing driver intention via hierarchical perception-action modeling," *IEEE Trans. Hum.-Mach. Syst.*, vol. 43, no. 1, pp. 17–31, Jan. 2013.
[78] D. M. Wolpert, J. Diedrichsen, and J. R. Flanagan, "Principles of sensorimotor learning," *Nat. Rev. Neurosci.*, vol. 12, no. 12, pp. 739–51, Dec. 2011.
[79] P. M. Bays and D. M. Wolpert, "Computational principles of sensorimotor control that minimize uncertainty and variability," *J. Physiol.*, vol. 578, pt. 2, pp. 387–96, Jan. 2007.
[80] Y. Demiris and B. Khadhouri, "Content-based control of goal-directed attention during human action perception," *Interact. Stud.*, vol. 9, no. 2, pp. 353–376, 2008.
[81] T. Carlson and Y. Demiris, "Collaborative control for a robotic wheelchair: Evaluation of performance, attention, workload," *IEEE Trans. Syst., Man, Cybern. B, Cybern.*, vol. 42, no. 3, pp. 876–888, Jan. 2012.
[82] E. Todorov, "Optimality principles in sensorimotor control," *Nat. Neurosci.*, vol. 7, no. 9, pp. 907–15, Sep. 2004.
[83] D. Liu and E. Todorov, "Evidence for the flexible sensorimotor strategies predicted by optimal feedback control," *J. Neurosci. Off. J. Soc. Neurosci.*, vol. 27, no. 35, pp. 9354–68, Aug. 2007.
[84] E. Todorov and M. I. Jordan, "Optimal feedback control as a theory of motor coordination," *Nat. Neurosci.*, vol. 5, no. 11, pp. 1226–1235, Nov. 2002.
[85] A. J. Nagengast, D. A. Braun, and D. M. Wolpert, "Optimal control predicts human performance on objects with internal degrees of freedom," *PLoS Comput. Biol.*, vol. 5, no. 6, p. e1000419, Jun. 2009.
[86] C. M. Harris, "Biomimetics of human movement: Functional or aesthetic?" *Bioinspir. Biomim.*, vol. 4, no. 3, p. 033001, Sep. 2009.
[87] C. M. Harris, "Signal-dependent noise determines motor planning," *Nature*, vol. 394, no. 6695, pp. 780–784, Aug. 1998.
[88] P. Viviani and T. Flash, "Minimum-jerk, two-thirds power law, isochrony: Converging approaches to movement planning," *J. Exp. Psychol. Hum. Percept. Perform.*, vol. 21, no. 1, pp. 32–53, Mar. 1995.
[89] H. Hicheur, S. Vieilledent, M. J. E. Richardson, T. Flash, and A. Berthoz, "Velocity and curvature in human locomotion along complex curved paths: A comparison with hand movements," *Exp. Brain Res.*, vol. 162, no. 2, pp. 145–54, Apr. 2005.
[90] T. Flash and B. Hochner, "Motor primitives in vertebrates and invertebrates," *Curr. Opin. Neurobiol.*, vol. 15, no. 6, pp. 660–6, Dec. 2005.
[91] T. Flash, Y. Meirovitch, and A. Barliya, "Models of human movement: Trajectory planning and inverse kinematics studies," *Robot. Auton. Syst.*, vol. 61, no. 4, pp. 330–339, Apr. 2013.
[92] A. Simpkins and E. Todorov, "Complex object manipulation with hierarchical optimal control," in *Proc. IEEE Symp. ADPRL*, 2011 pp. 338–345.
[93] E. Todorov and M. I. Jordan, "A minimal intervention principle for coordinated movement," in *Proc. Adv. Neural Inf. Process. Syst.*, 2003, vol. 15, pp. 27–34.
[94] F. J. Valero-Cuevas, M. Venkadesan, and E. Todorov, "Structured variability of muscle activations supports the minimal intervention principle of motor control," *J. Neurophysiol.*, vol. 102, no. 1, pp. 59–68, Jul. 2009.
[95] R. S. Rice, "Measuring car-driver interaction with the g-g diagram," presented at the SAE International Automotive Engineering Congress, Detroit, MI, USA, 1973, SAE Tech. Paper 730018.
[96] Y. Hisaoka, M. Yamamoto, and A. Okada, "Closed-loop analysis of vehicle behavior during braking in a turn," *JSAE Rev.*, vol. 20, no. 4, pp. 537–542, Oct. 1999.
[97] W. Bartlett, O. Masory, and B. Wright, "Driver abilities in closed course testing," presented at the SAE World Congress, Detroit, MI, USA, 2000, SAE Tech. Paper 2000-01-0179.
[98] P. Bosetti, M. Da Lio, and A. Saroldi, "On the human control of vehicles: An experimental study of acceleration," *Eur. Transp. Res. Rev.*, vol. 6, no. 2, pp. 157–170, Jun. 2013.
[99] interactIVe-Accident avoidance by intervention for Intelligent Vehicles, [Accessed: 30-May-2013]. [Online]. Available: http://www.interactive-ip.eu/
[100] M. Abe, *Vehicle Handling Dynamics*. Oxford, U.K.: Elsevier, 2009, p. 286.
[101] H. Moriguchi and H. Lipson, "Learning symbolic forward models for robotic motion planning and control," in *Proc. ECAL*, 2011, pp. 558–564.
[102] D. Nguyen-Tuong, M. Seeger, and J. Peters, "Real-time local GP model learning," in *From Motor Learning to Interaction Learning in Robots*, vol. 264, *Studies in Computational Intelligence*. Berlin, Germany: Springer-Verlag, 2010, pp. 193–207.
[103] D. Nguyen-Tuong and J. Peters, "Local Gaussian process regression for real-time model-based robot control," in *Proc. IEEE/RSJ IROS*, 2008, pp. 380–385.
[104] D. Nguyen-Tuong and J. Peters, "Model learning for robot control: A survey," *Cogn. Process.*, vol. 12, no. 4, pp. 319–340, Nov. 2011.
[105] O. Sigaud, C. Salan, and V. Padois, "On-line regression algorithms for learning mechanical models of robots: A survey," *Robot. Auton. Syst.*, vol. 59, no. 12, pp. 1115–1129, Dec. 2011.
[106] B. Bócsi, P. Hennig, L. Csató, and J. Peters, "Learning tracking control with forward models," in *Proc. IEEE Int. Conf. Robot. Autom.*, 2012, pp. 259–264.
[107] S. Kim and A. Billard, "Estimating the non-linear dynamics of free-flying objects," *Robot. Auton. Syst.*, vol. 60, no. 9, pp. 1108–1122, Sep. 2012.
[108] A. Gijsberts and G. Metta, "Real-time model learning using incremental sparse spectrum Gaussian process regression," *Neural Netw.*, vol. 41, pp. 59–69, May 2013.
[109] D. Mitrovic, S. Klanke, and S. Vijayakumar, "Adaptive optimal feedback control with learned internal dynamics models," in *From Motor Learning to Interaction Learning in Robots*, vol. 264. Berlin, USA: Springer-Verlag, 2010, pp. 65–84.
[110] D. Mitrovic, S. Klanke, and S. Vijayakumar, "Adaptive optimal control for redundantly actuated arms," in *From Animals to Animats 10*, vol. 5040. Berlin, USA: Springer-Verlag, 2008, ser. Lecture Notes in Computer Science, pp. 93–102.
[111] S. Vijayakumar, A. D'Souza, and S. Schaal, "Incremental online learning in high dimensions," *Neural Comput.*, vol. 17, no. 12, pp. 2602–2634, Dec. 2005.
[112] F. Larsson, E. Jonsson, and M. Felsberg, "Simultaneously learning to recognize and control a low-cost robotic arm," *Image Vis. Comput.*, vol. 27, no. 11, pp. 1729–1739, Oct. 2009.
[113] S. G. Khan, G. Herrmann, F. L. Lewis, T. Pipe, and C. Melhuish, "Reinforcement learning and optimal adaptive control: An overview and implementation examples," *Annu. Rev. Control*, vol. 36, no. 1, pp. 42–59, Apr. 2012.

[114] S. Schaal and C. G. Atkeson, "Learning control in robotics," *IEEE Robot. Autom. Mag.*, vol. 17, no. 2, pp. 20–29, Jun. 2010.
[115] A. G. Barto and R. S. Sutton, "Reinforcement learning in artificial intelligence," *Adv. Psychol.*, vol. C-121, pp. 358–386, 1997.
[116] R. S. Sutton, A. G. Barto, and R. J. Williams, "Reinforcement learning is direct adaptive optimal control," *IEEE Control Syst. Mag.*, vol. 12, no. 2, pp. 19–22, Apr. 1992.
[117] E. Bertolazzi, F. Biral, and M. Da Lio, "Symbolic-numeric efficient solution of optimal control problems for multibody systems," *J. Comput. Appl. Math.*, vol. 185, no. 2, pp. 404–421, Jan. 2006.
[118] E. Bertolazzi, F. Biral, and M. Da Lio, "Real-time motion planning for multibody systems: Real life application examples," *Multibody Syst. Dyn.*, vol. 17, no. 2/3, pp. 119–139, Apr. 2007.
[119] E. Bertolazzi, F. Biral, and M. Da Lio, "Symbolic-numeric indirect method for solving optimal control problems for large multibody systems: The time-optimal racing vehicle example," *Multibody Syst. Dyn.*, vol. 13, no. 2, pp. 233–252, 2005.
[120] F. Biral *et al.*, "A web based 'Virtual Racing Car Championship' to teach vehicle dynamics and multidisciplinary design," in *Proc. ASME IMECE*, 2011, vol. 5, pp. 391–401.
[121] B. Hommel, J. Müsseler, G. Aschersleben, and W. Prinz, "The Theory of Event Coding (TEC): A framework for perception and action planning," *Behav. Brain Sci.*, vol. 24, no. 5, pp. 849–878, Oct. 2001, discussion 878–937.
[122] A. M. Liberman and I. G. Mattingly, "The motor theory of speech perception revised," *Cognition*, vol. 21, no. 1, pp. 1–36, Oct. 1985.
[123] B. Galantucci, C. A. Fowler, and M. T. Turvey, "Event coding as feature guessing: The lessons of the motor theory of speech perception," *Behav. Brain Sci.*, vol. 24, no. 5, pp. 886–887, Oct. 2001.
[124] A. Doshi and M. M. Trivedi, "Tactical driver behavior prediction and intent inference: A review," in *Proc. IEEE ITSC*, 2011, pp. 1892–1897.
[125] F. Lethaus, M. R. K. Baumann, F. Köster, and K. Lemmer, "A comparison of selected simple supervised learning algorithms to predict driver intent based on gaze data," *Neurocomputing*, vol. 121, pp. 108–130, Dec. 2013.
[126] G. Csibra and G. Gergely, "'Obsessed with goals': Functions and mechanisms of teleological interpretation of actions in humans," *Acta Psychol. (Amst.)*, vol. 124, no. 1, pp. 60–78, Jan. 2007.
[127] J. C. McCall, D. P. Wipf, M. M. Trivedi, and B. D. Rao, "Lane change intent analysis using robust operators and sparse Bayesian learning," *IEEE Trans. Intell. Transp. Syst.*, vol. 8, no. 3, pp. 431–440, Sep. 2007.
[128] D. Windridge and J. Kittler, "Perception-action learning as an epistemologically-consistent model for self-updating cognitive representation," *Adv. Exp. Med. Biol.*, vol. 657, pp. 95–134, 2010.
[129] M. Shevchenko, D. Windridge, and J. Kittler, "A linear-complexity reparameterisation strategy for the hierarchical bootstrapping of capabilities within perception-action architectures," *Image Vis. Comput.*, vol. 27, no. 11, pp. 1702–1714, Oct. 2009.
[130] V. Cossalter, M. Da Lio, R. Lot, and L. Fabbri, "A general method for the evaluation of vehicle manoeuvrability with special emphasis on motorcycles," *Veh. Syst. Dyn.*, vol. 31, no. 2, pp. 113–135, 1999.

Mauro Da Lio (M'10) received the Laurea degree in mechanical engineering from University of Padova, Padova, Italy, in 1986.

He is a Full Professor of mechanical systems with University of Trento, Trento, Italy. He was with an offshore oil research company in underwater robotics (EUREKA project). He has been involved in several EU framework programme 6 and 7 projects (PReVENT, SAFERIDER, interactIVe, VERITAS, adaptIVe, and NoTremor). His earlier research activity was on modeling, simulation, and optimal control of mechanical multibody systems, particularly vehicle and spacecraft dynamics. More recently, his focus has shifted to the modeling of human sensory-motor control, particularly drivers and motor-impaired people.

Francesco Biral received the Laurea degree in mechanical engineering from University of Padova, Padova, Italy, in 1997 and the Ph.D. degree in mechanism and machine theory from University of Brescia, Brescia, Italy, in 2000.

He is an Associate Professor with University of Trento, Trento, Italy. His research interests include multibody dynamics and optimization, constrained optimal control, model-predictive control, smart manufacturing systems, and motorcycle and automotive applications of safety systems and automatic control.

Enrico Bertolazzi received the Laurea degree in mathematics from University of Trento, Trento, Italy, in 1990.

He is an Associate Professor with University of Trento. He was with a small company developing numerical algorithm for computer-aided manufacturing. His research interests include numerical analysis and finite volumes for convective dominated and hypersonic flow, discrete maximum principle, constrained optimal control, and scientific programming.

Marco Galvani received the B.S. degree in industrial engineering, the M.S. degree in mechatronic engineering, and the Ph.D. degree in engineering of civil and mechanical structural systems from University of Trento, Trento, Italy, in 2006, 2009, and 2013, respectively.

During his studies, he spent some months researching at Volvo Technology AB, Gothenburg, Sweden, and at the Hori-Fujimoto Laboratory, University of Tokyo, Tokyo, Japan. His research interests include vehicle and driver modeling, optimal control, and advanced driver assistance system development.

Paolo Bosetti received the Laurea degree in materials engineering and the Ph.D. degree in materials and structural engineering from University of Trento, Trento, Italy, in 1997 and 2002, respectively.

He is an Assistant Professor with the Department of Industrial Engineering, University of Trento, where he is in charge of the courses on manufacturing automation, manufacturing process design, and design of manufacturing systems. His research interests include mechatronic systems, automation, and smart manufacturing systems.

David Windridge received a B.Sc. in Physics from the University of Durham, UK, in 1993, a M.Sc. in Radio Astronomy from the University of Manchester, UK, in 1995, and a Ph.D in Astrophysics from the University of Bristol, UK in 1999.

He is a Senior Research Fellow with University of Surrey, Surrey, U.K. He has authored more than 70 peer-reviewed publications. His grant portfolio includes a range of EPSRC and EU cognitive systems projects (including EPSRC ACASVA and EU FP7 DIPLECS), as well as a number of industrial and academic pattern recognition projects. His former research interest was astronomy/astrophysics and his current research interests include pattern recognition and cognitive systems.

Andrea Saroldi received the Laurea degree in physics from University of Turin, Turin, Italy, in 1985.

Since 1986, he has been with Centro Ricerche Fiat, Orbassano, Italy, as part of a group involved with advanced driver assistance systems. He has been the Project Leader for subproject SASPENCE of the PReVENT Integrating Project and for subproject SECONDS of the interactIVe Integrated Project. His research interests are in processing of sensor data and development of driver assistance functions for preventive safety.

Fabio Tango received the Laurea degree in physics (solid state) and the Ph.D. degree in computer science from University of Turin, Turin, Italy, in 1995 and 2009, respectively.

Since 1999, he has been with Centro Ricerche Fiat, Orbassano, Italy, in the ADAS department, where he researches preventive safety systems. His topics of interest include human–computer interaction modeling, pattern recognition and analysis, data fusion and object classification, and applications in image processing.